AN INVESTIGATION OF SECONDARY FLOW EFFECTS IN CURVED CHANNELS OF SQUARE CROSS SECTION

Paul Stephen Kenney

NAVAL POSTGRADUATE SCHOOL
Monterey, California

THESIS

An Investigation of Secondary Flow Effects in Curved Channels of Square Cross Section

by

Paul Stephen Kenney

Thesis Advisor: M. H. Vavra

June 1973

An Investigation of Secondary Flow Effects In Curved Channels of Square Cross Section

by

Paul Stephen Kenney
Ensign, United States Navy
B.S., United States Naval Academy, 1972

Submitted in partial fulfillment of the
requirements for the degree of

MASTER OF SCIENCE IN AERONAUTICAL ENGINEERING

from the

NAVAL POSTGRADUATE SCHOOL
June 1973

ABSTRACT

In this study, turbulent flow in a curved channel of square cross section was investigated experimentally to determine secondary flow effects. Probe surveys were conducted to establish vortex and total pressure loss distribution in the exit plane of a 90° bend. Overall losses were determined by measuring the momentum of the flow with a force plate for different Reynolds numbers at turning angles of 0°, 45°, 90°, and 135°.

TABLE OF CONTENTS

LIST OF FIGURES

ACKNOWLEDGEMENT

The author is most grateful for the instruction and guidance received from Dr. M. H. Vavra throughout the course of this study. The technicians of the Aeronautics Department, especially Mr. J. Hammer, are acknowledged for their assistance in constructing and operating experimental equipment.

I. INTRODUCTION

The art of designing turbomachines has improved radically during the past decades. A better understanding of flow conditions in rotors and stators has been responsible for much of this improvement. Continued advancement in turbomachinery cannot be achieved without an increased knowledge of flow patterns and conditions which exist in various blade configurations.

An important flow phenomenon known to exist but not too well understood is that of secondary flow produced when flow is directed between the curved surfaces of adjacent blades in a cascade. Losses caused by secondary flow reduce the efficiency of turbomachines. A better understanding of these losses may result in establishing design techniques to minimize them.

The purpose of this study was to investigate secondary flow effects produced when a turbulent flow is directed through a curved channel of square cross section. As shown in Figure 1, the vertical walls of the channel represent the surfaces of adjacent blades in a cascade. Procedures required to investigate secondary flow in a cascade test rig are complicated, and the distinguishing of secondary flow effects from tip effects, trailing vortices, and wakes can be very difficult. The simple model of Figure 1 eliminates many of these complications.

Probe surveys were conducted to investigate the flow field at the exit of a 90° bend. Overall secondary flow losses were determined for bends with different turning angles by using a force plate to measure the useful exit momentum. To accomplish this, a hydraulic force plate apparatus was designed.

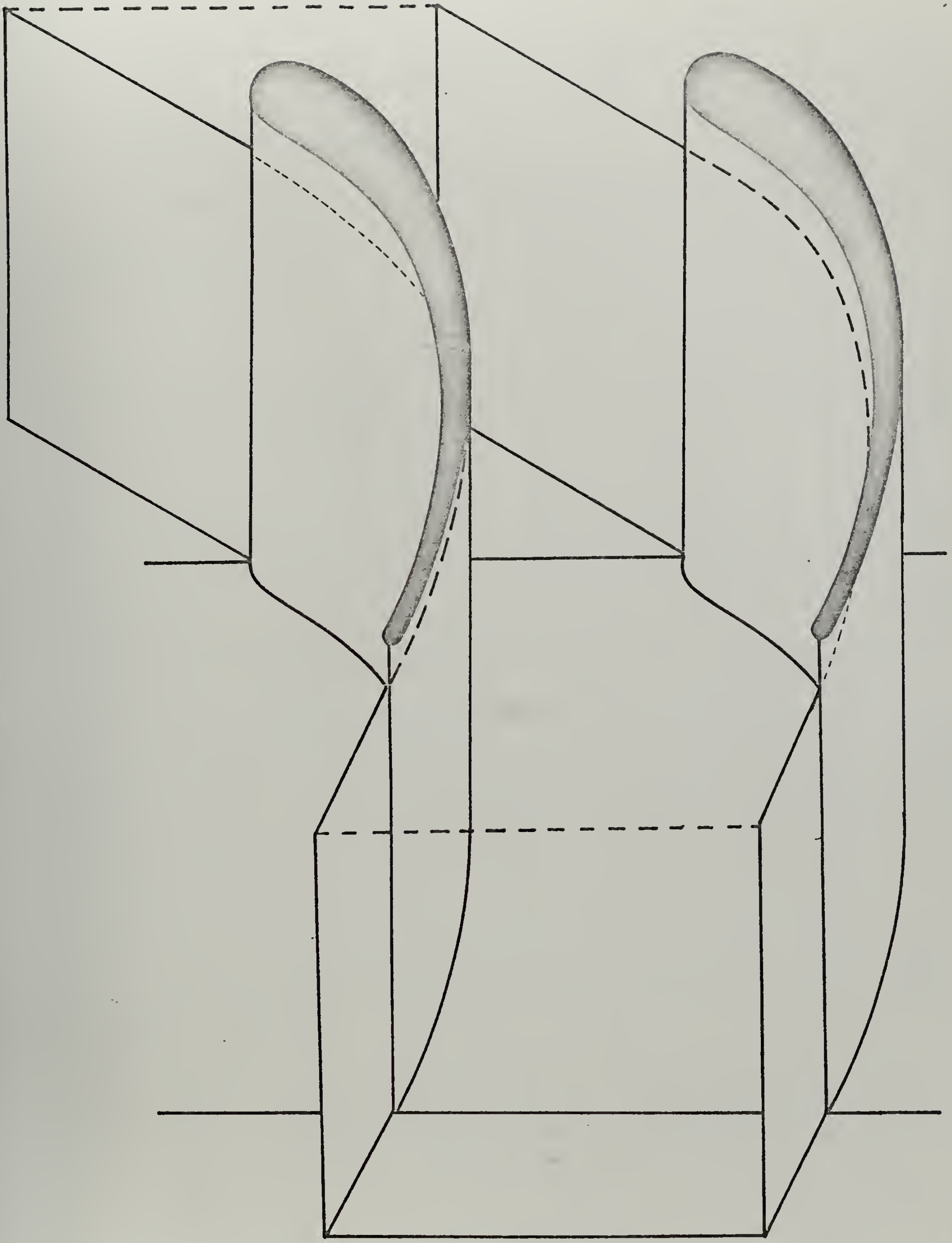

Figure 1

Representation of Adjacent Blade Surfaces by a Square Channel

II. APPROACH TO PROBLEM

A. SECONDARY FLOW EFFECTS

The results of applying the equation of motion for incompressible flow

$$\nabla\left(\frac{P}{\rho}\right) = \vec{V} \times (\nabla \times \vec{V})$$

to flow passing through a rectangular curved channel is taken from Vavra [Ref. 1] and shown in Figure 2. The vortices represent the well known secondary flow. Losses associated with secondary flow can be separated into two categories.

Flow in a straight channel has total pressure losses. For the flow velocities and channel size being considered, these losses tend to be confined to the boundary layer regions along the walls and in the corners. In curved channels, secondary flow vortices distribute boundary layer flow throughout the channel. This results in a higher total pressure loss for a curved channel than for a straight channel.

The second type of loss is due to angular deflection of the flow in different directions. The direction of the overall path of the flow is obtained by averaging individual particle velocities over the channel cross section. Velocity components perpendicular to the overall flow path are produced by secondary flow. In the blading of turbomachines, these velocity components do not contribute to

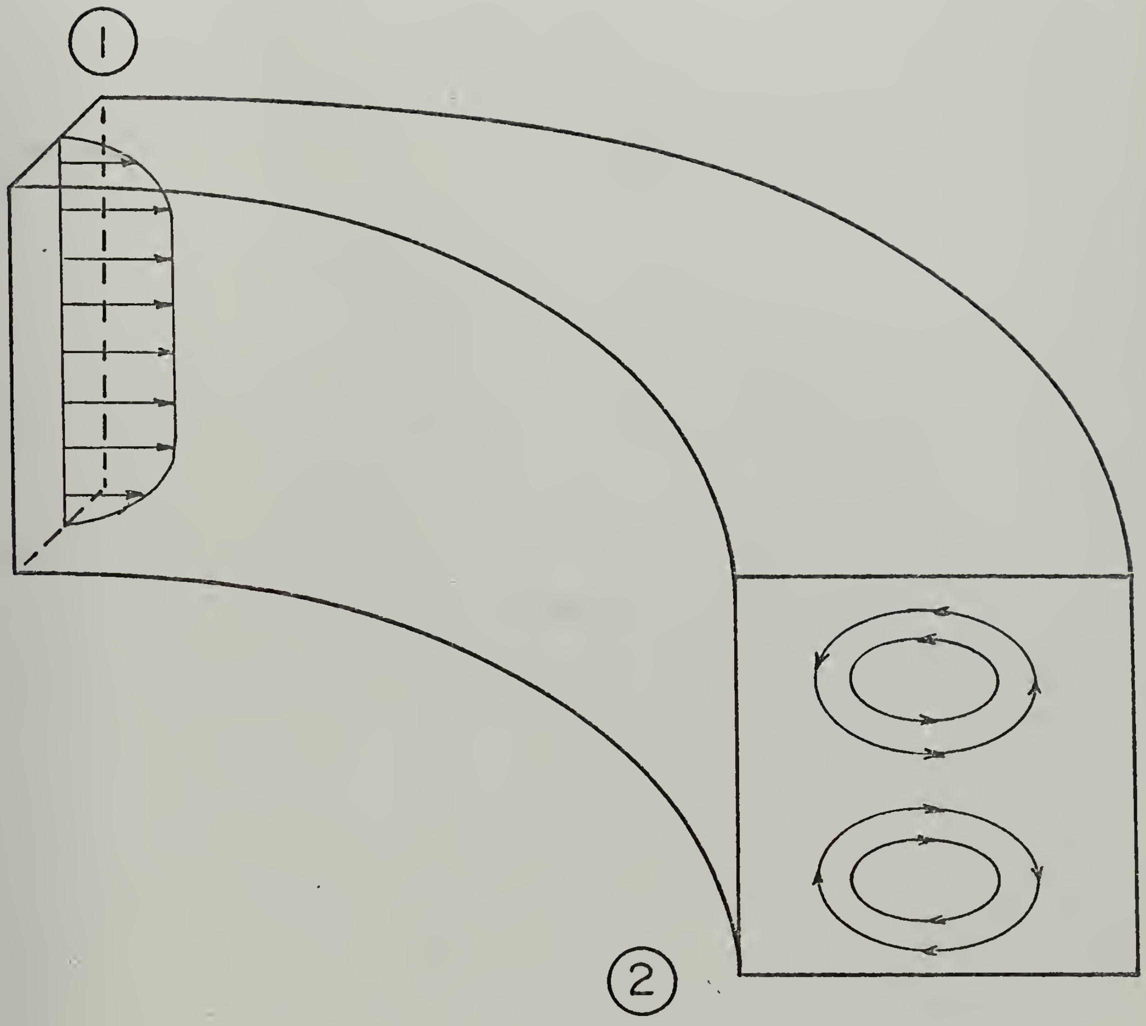

Figure 2
Secondary Flow Vortices in a Rectangular Bend

the energy conversion in the machine and can be classified as non-useful.

Analytical treatments of secondary flows in turbomachines were done in Ref. 3. It was concluded that no method was available to adequately predict losses caused by secondary flow. It is desirable, therefore, to investigate and measure these losses in well controlled experiments.

B. FORCE PLATE DETERMINATION OF LOSSES

An isentropic process from uniform conditions at station 1 to station 2 of Figure 2 would yield an exit velocity of $V_{2_{th}}$. A process with total pressure losses between 1 and 2 would yield an average velocity V_2, which is smaller than $V_{2_{th}}$. The difference between V_2 and $V_{2_{th}}$ increases with increasing loss. The velocity distribution at station 2 can be determined by probe surveys. A complete survey would be required for each turning angle and flow rate investigated. The impact force of the flow at station 2 is directly related to its average velocity. A large plate positioned perpendicular to the flow path as shown in Figure 3 serves to measure the impact force of the flow. Such a plate measures only the velocity components parallel to the flow path, thus eliminating the non-useful velocities. Conservation of momentum is applied to the control volume shown in Figure 3. The flow enters the control volume through surface 2 and is assumed to exit

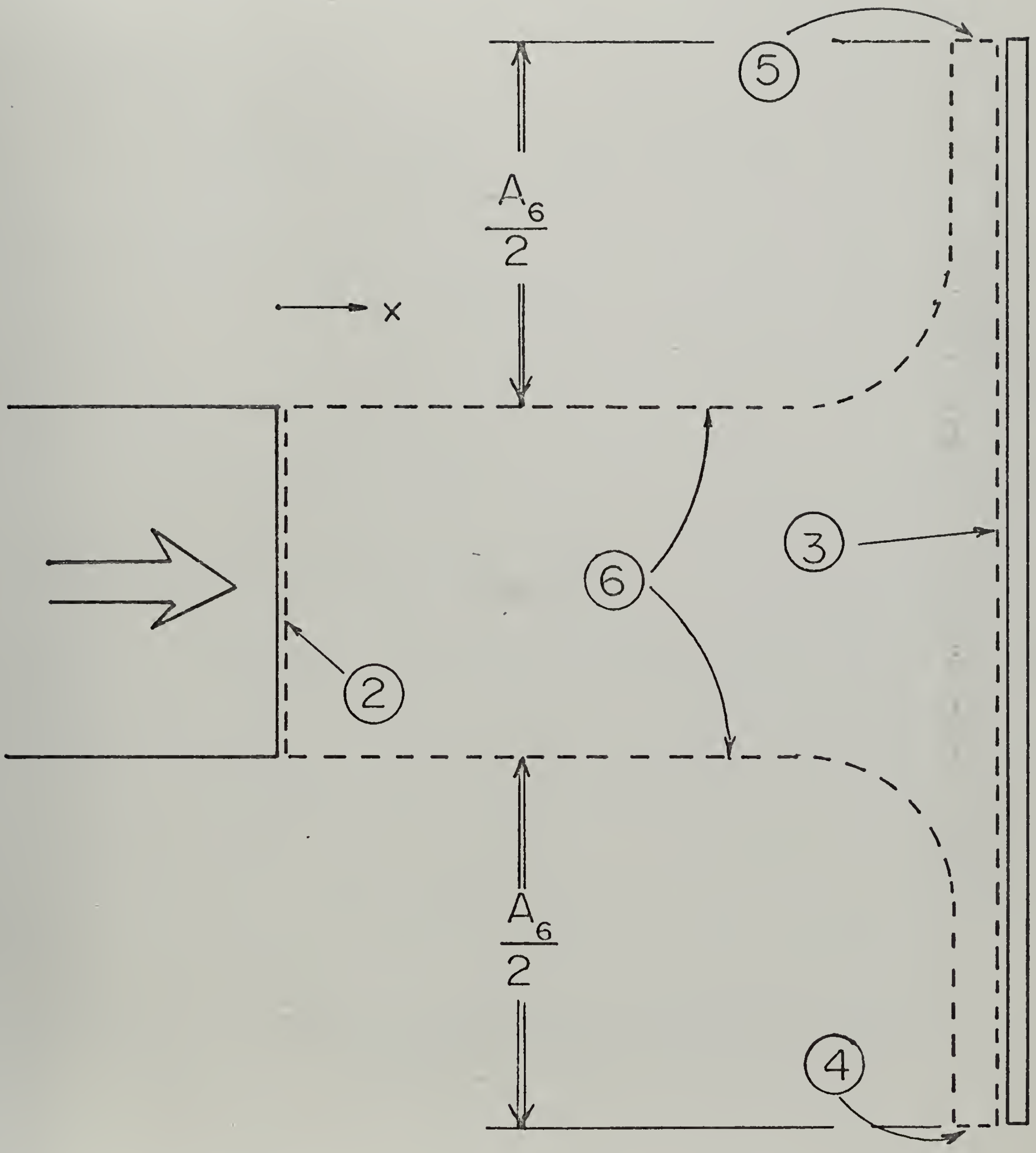

Figure 3

Conservation of Momentum Applied to the Force Plate

perpendicularly through control surfaces 4 and 5. The static pressure along surface 6 is assumed to be atmospheric (P_A). The force on the control volume in the x-direction must be equal to the change of momentum in the x-direction. Thus

$$-\int_{A_2} \rho V_x^2 dA = \int_{A_2} P_2 dA - \int_{A_3} P_3 dA + \int_{A_6} P_A dA \qquad (1)$$

The force on the plate, F, is given by

$$F = \int_{A_3} P_3 dA - P_A A_3 \qquad (2)$$

or,

$$\int_{A_3} P_3 dA = F + P_A A_3$$

Substituting this relation into (1)

$$-\int_{A_2} \rho V_x^2 dA = \int_{A_2} P_2 dA - [F + P_A A_3] + P_A A_6$$

$$-\int_{A_2} \rho V_x^2 dA = \int_{A_2} P_2 dA - F + P_A (A_6 - A_3)$$

$$F = \int_{A_2} \rho V_x^2 dA + \int_{A_2} P_2 dA - P_A A_2$$

$$F = \int_{A_2} \rho V_x^2 dA + \int_{A_2} (P_2 - P_A)\, dA \qquad (3)$$

Probe and pressure tap measurements indicated that P_2 was equal to P_A within 0.06 inches of water in all experiments using the force plate. Based on this experience, P_2 was assumed to be equal to P_A . Equation (3) then becomes

$$F = \int_{A_2} \rho V_x^2 dA$$

A loss coefficient is defined in Appendix A using force plate measurements.

C. PROBE SURVEY OF THE FLOW FIELD

Determination of secondary losses is important in identifying their magnitude in channels with different turning angles and Reynolds numbers. A better understanding of the secondary flow phenomena may be achieved if these measurements are combined with probe surveys of the flow field at the channel exit. The secondary flow vortices shown in Figure 2 are the result of theoretical analysis. The actual location of vortices can be determined only by experiment.

III. DESIGN OF FORCE PLATE APPARATUS

A. PRELIMINARY CONSIDERATIONS

An apparatus was needed to measure the force exerted on the force plate by the flow. A hydraulic apparatus was devised for this purpose which is shown in Figure 4. The force plate is directly connected to the piston and the oil in the cylinder is assumed to be incompressible. Any change in the force F will result in an instantaneous change in P_1. The leakage at A_2 represents the piston-cylinder leakage and is a function of P_1. If P_1 increases, leakage through A_2 increases while flow through A_1 decreases. Hence the volume of oil in the cylinder decreases, causing the piston to move in the y-direction. As the piston moves, the valve at A_1 opens, admitting more oil to the cylinder to compensate for the higher leakage. The interactions are the same but reversed if F decreases. Three considerations which lead to the final design are discussed in the sections which follow.

1. Stability

Before establishing a mechanical design, the system of Figure 4 was investigated for stability. At any instant, the flow rate through A_1 must equal the flow rate through A_2 plus the rate of increase in system volume. Hence

$$\frac{dy}{dt} + y\,H(t) = Q(t) \qquad (5)$$

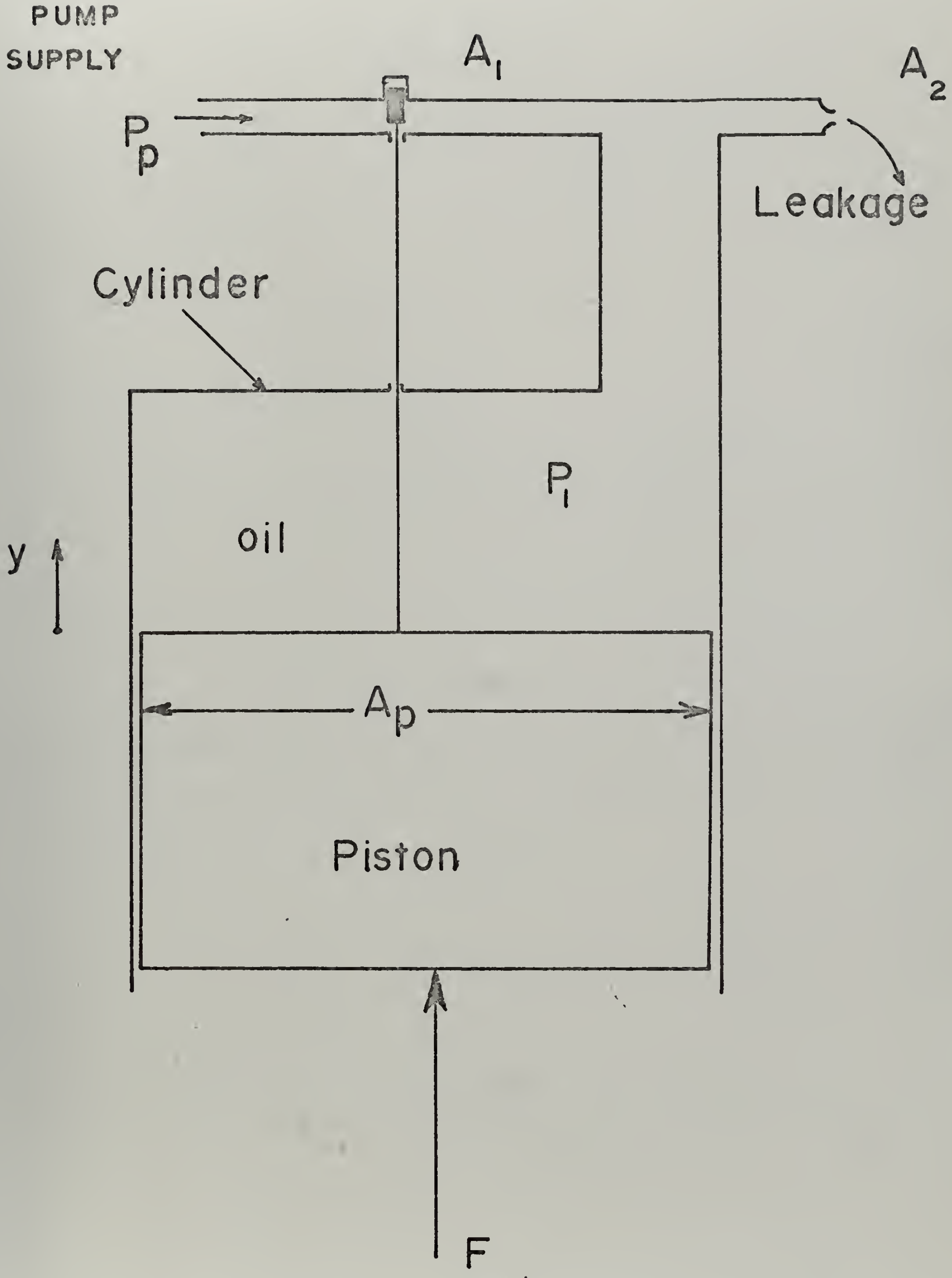

Figure 4
Operating Principle of Hydraulic Force Plate Apparatus

where

$$H(t) = \left[\frac{w}{A_p} \sqrt{\frac{2(P_p - P_1)}{\rho}} \right]$$

$$Q(t) = \frac{A_2}{A_p} \sqrt{\frac{2P_1}{\rho}} - \frac{wy_0}{A_p} \sqrt{\frac{2(P_p - P_1)}{\rho}}$$

$$yw = A_1$$

$$y_0 = \frac{A_1}{w} \quad \text{when } t = 0$$

Equation (5) has the solution

$$y(t) = e^{-\int_0^t H(t)dt} \int_0^t Q(t)\, e^{\int_0^t H(t)dt}\, dt + C\, e^{-\int_0^t H(t)dt} \tag{6}$$

where

$$C = y_0$$

System response was evaluated for the following conditions and forced pressure variations. Solutions were obtained by numerical trapezoidal integration.

$P_1 = 0.203$ lb/in^2 for $t < 0$

$P_1 = P_0 + \lambda P_0 \sin(2\pi \frac{t}{T})$ for $t \geq 0$

$y_0 = 0.001$ in

$P_0 = 5.0$ lb/in^2

$\lambda = 0.5$

$w = 1.0$ in

$A_p = 4\pi$ in^2

$\rho = 0.921$ gm/cm^3 (Turbine Oil Esso 15)

$P_p = 200$ lb/in^2

$A_2 = 0.0314$ in^2

Case I: $T = 0.05$ sec

Case II: $T = 0.10$ sec

Case III: $T = 0.20$ sec

The results are shown in Figures 5 - 7. The disturbances at 0.25 seconds in Figure 5 and 0.07 seconds in Figure 6 were attributed to the numerical method used to solve Equation 6. From these results, the apparatus appeared to be stable.

2. Friction

After it was verified that the system was stable, a mechanical design was undertaken. The initial proposal is shown in Figure 8. Motion of the piston due to a change in F changes the amount of oil admitted from the pump. For each force applied, the piston moves to an equilibrium position such that the flow entering the cylinder equals the leakage flow. The stopper arrangement prevents the plate and piston from rotating.

Friction between the piston and cylinder decreases the measuring accuracy. Influences of static friction between piston and cylinder surfaces were eliminated by rotating the cylinder. The design of Figure 8 was modified to allow for cylinder rotation by a low-speed electric motor and is shown in Figure 9. The addition of oil grooves and outer housing were necessary to allow for cylinder rotation. Although the design of Figure 9 eliminated static friction, it increased the problem of leakage.

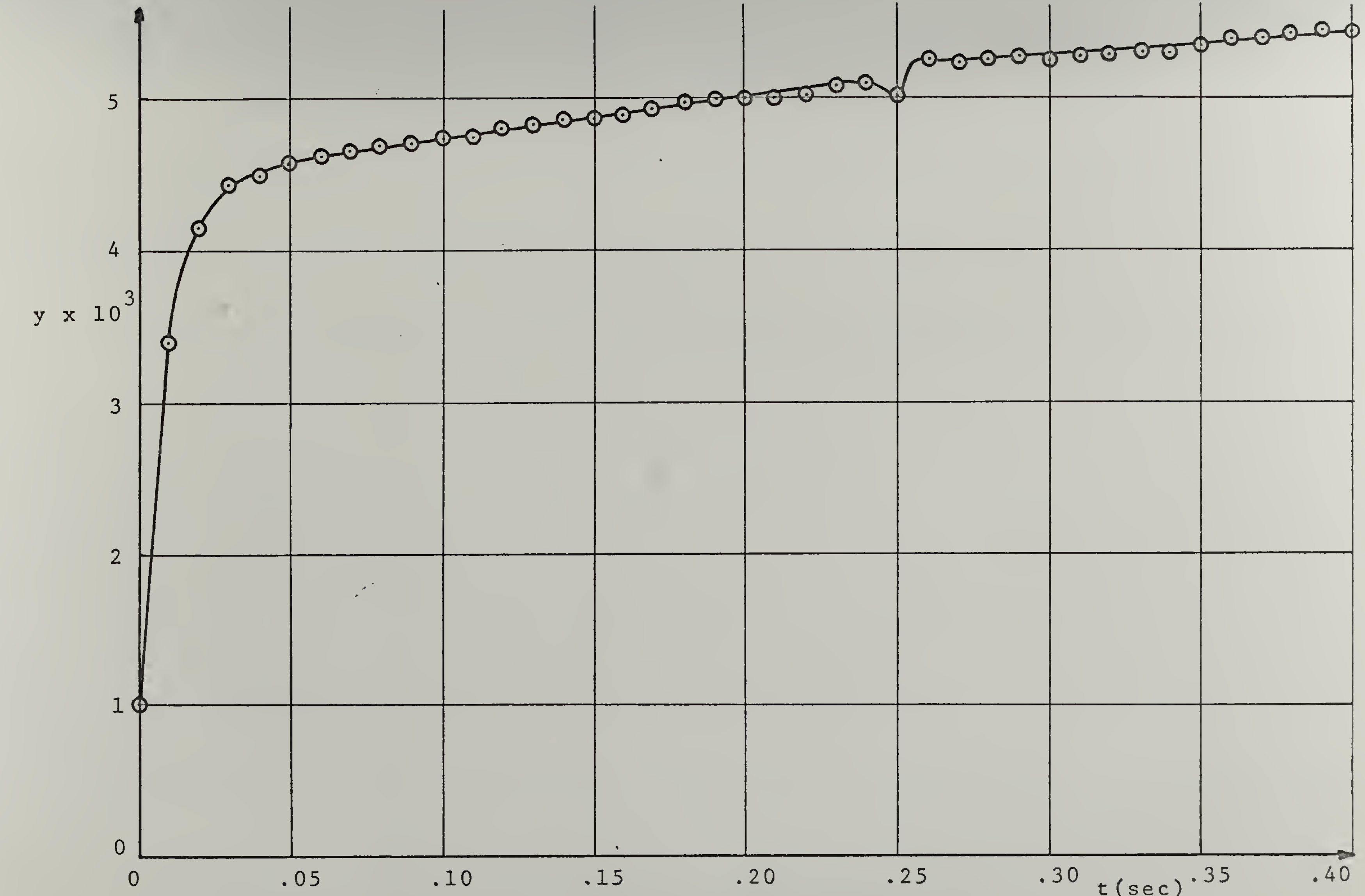

Figure 5. Piston motion "y" as a function of time "t" for Case I.

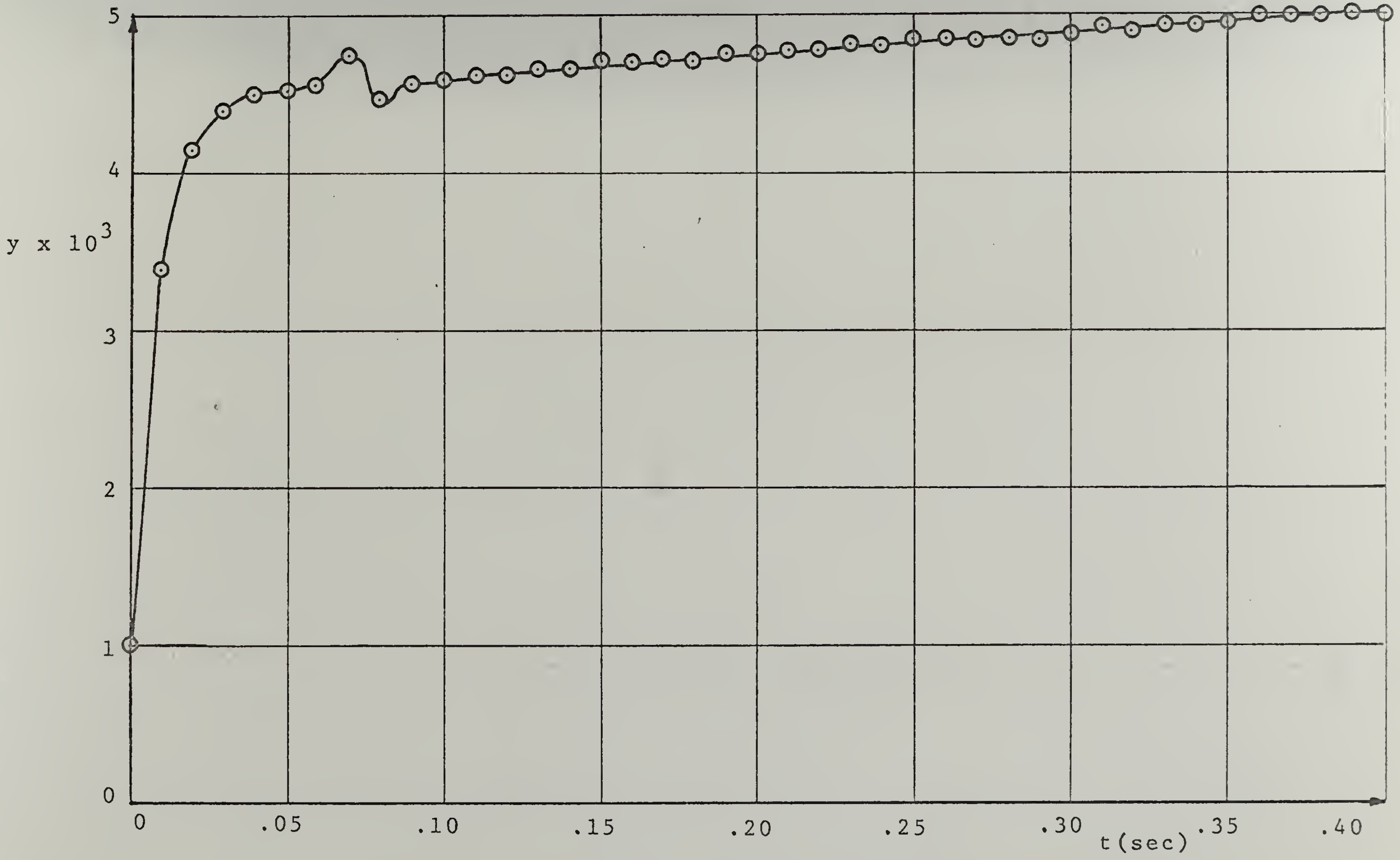

Figure 6

Piston motion for Case II

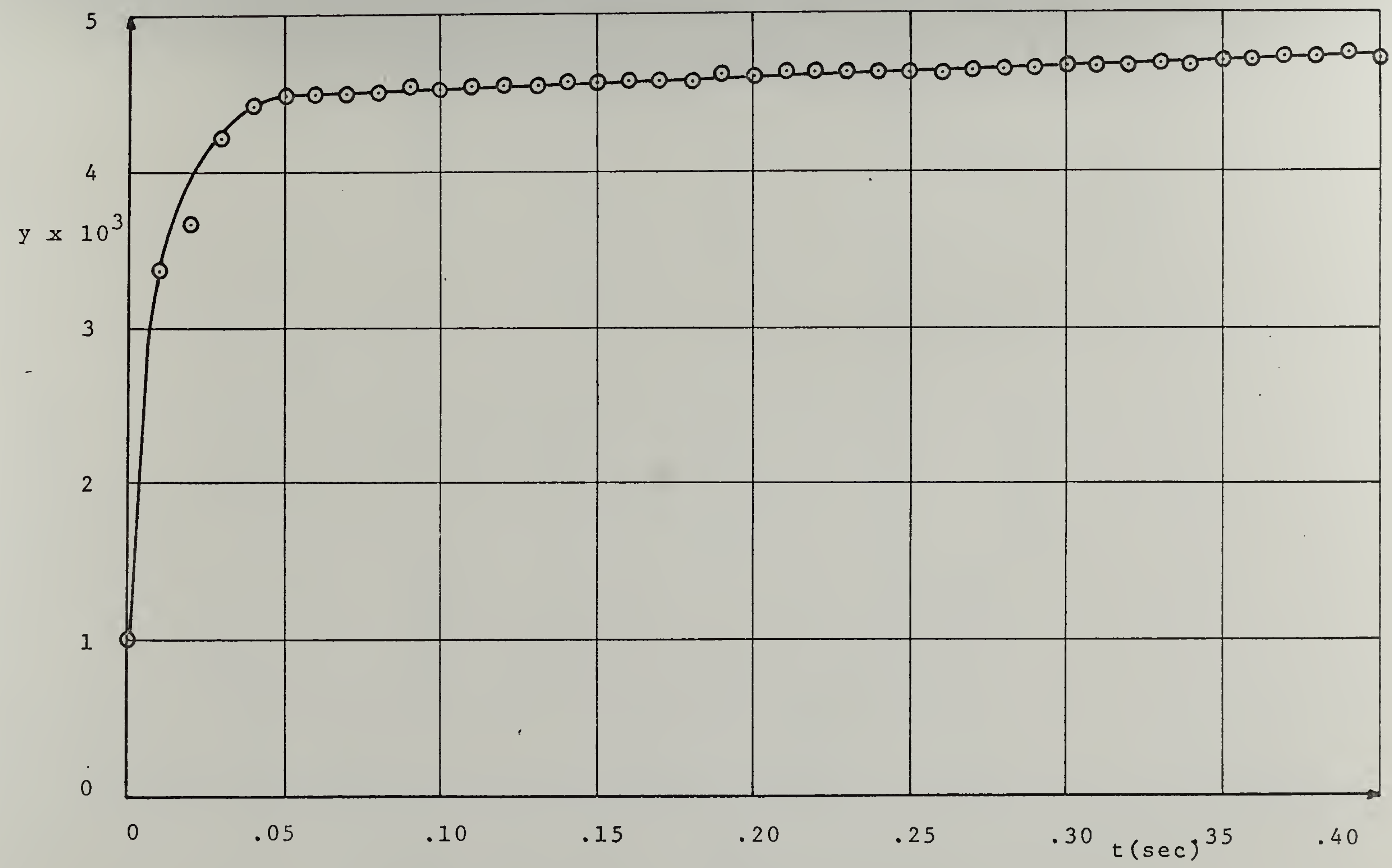

Figure 7

Piston motion for Case III

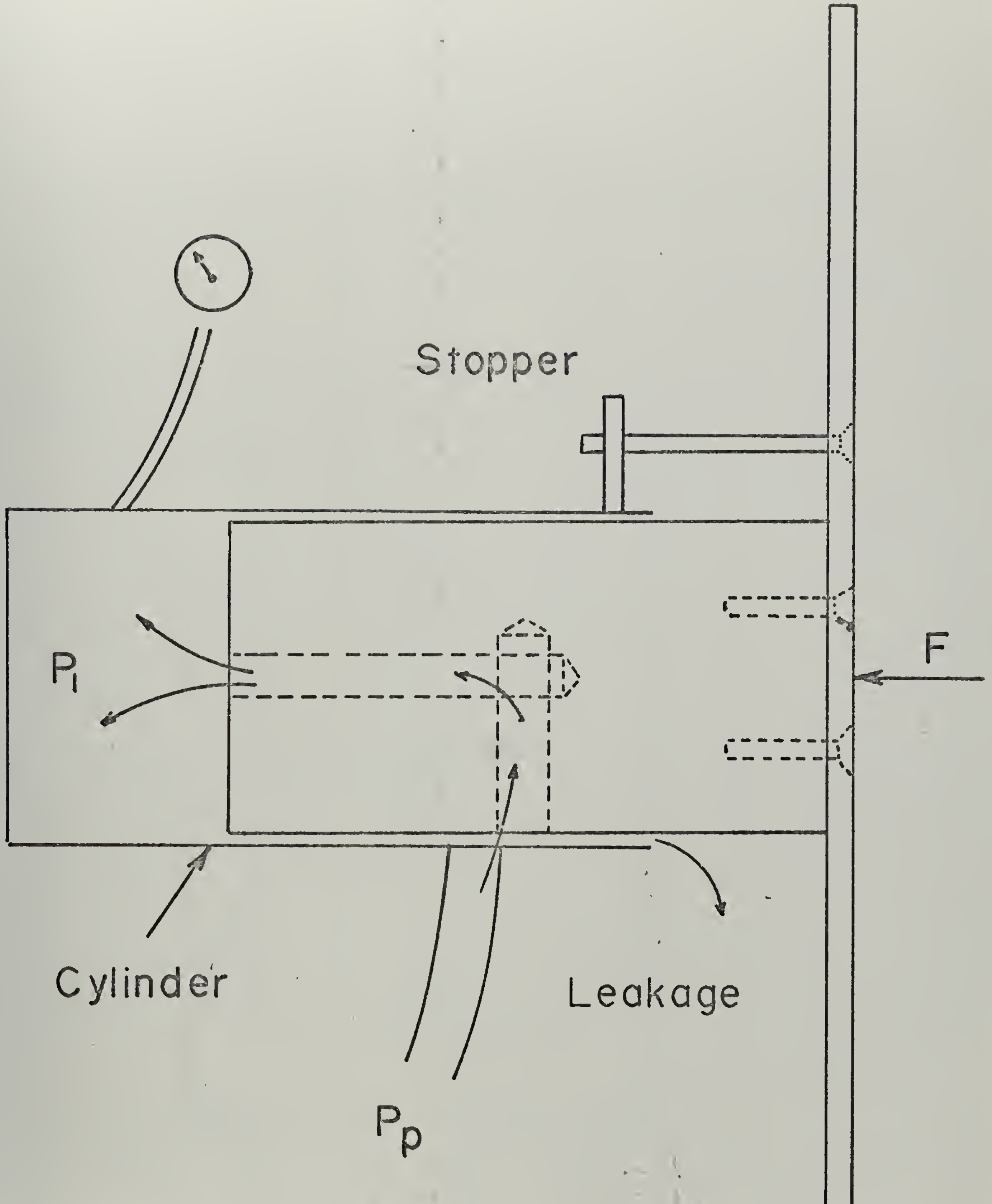

Figure 8

Original Design Configuration of the Force Plate Apparatus

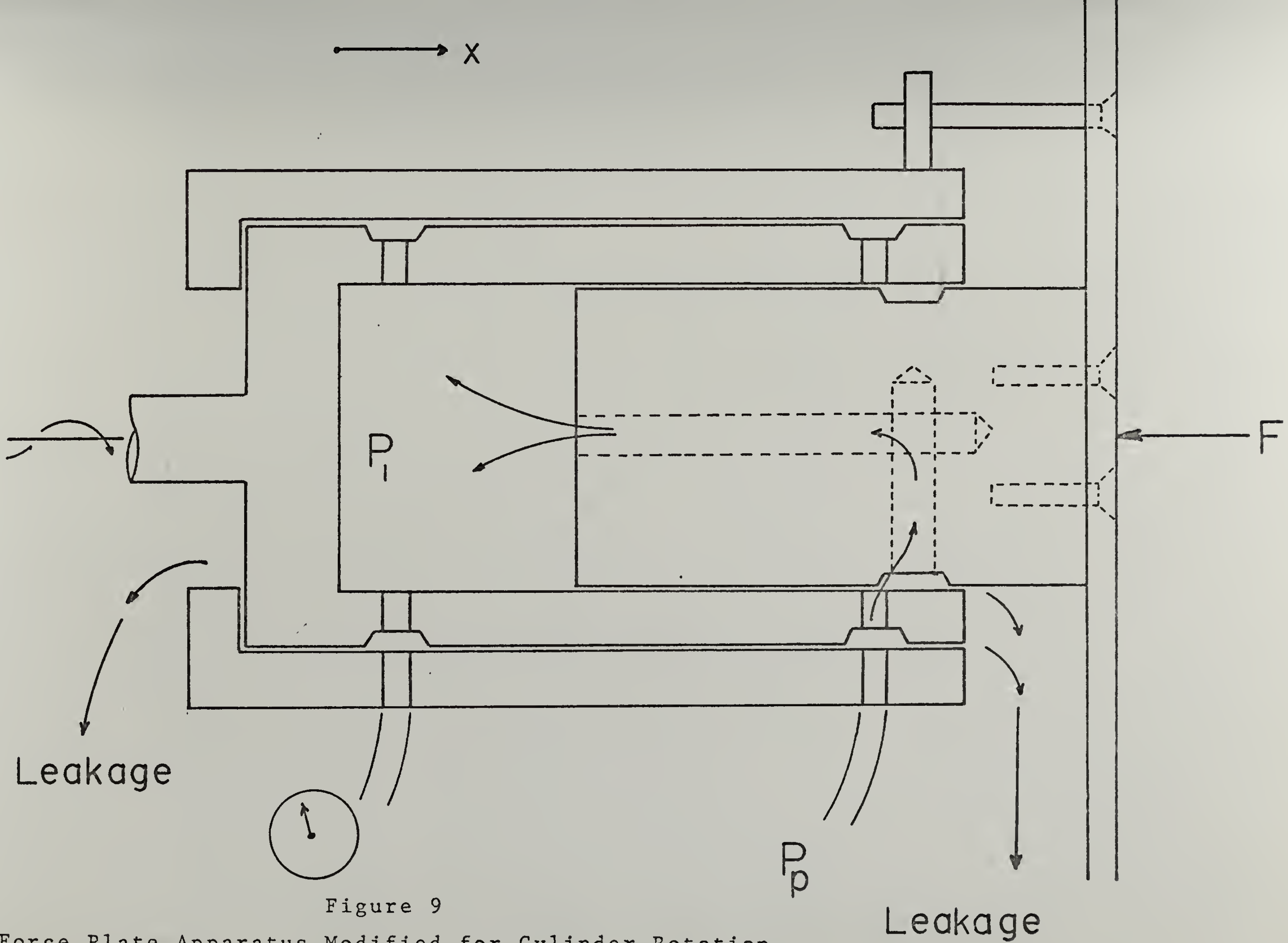

Figure 9
Force Plate Apparatus Modified for Cylinder Rotation

3. Leakage

Leakage between the piston and cylinder was necessary to provide proper lubrication in minimizing friction. Additional leakage between the cylinder and housing introduced by the design of Figure 9 was eliminated by O-ring seals as shown in Figure 10. Upon completion of the force plate apparatus, problems were encountered with proper O-ring sealing and are discussed in Appendix B.

B. FINAL DESIGN

These considerations, along with other factors, led to the final design of the force plate apparatus. The design drawings and photographs of the finished parts are shown in Figures 11 - 17. All parts were made at the Naval Postgraduate School, Monterey, California. Grades of steel specified on the drawings were not used. The piston was made of stainless steel whereas other parts were made of steel whose grades are not known exactly, to avoid delays associated with ordering specific materials.

The oil catcher photograph (Figure 15B) shows an addition not shown in the drawing. This device was welded in place after machining and connected to a suction pump for drainage purposes. The grease fittings in Figure 14A provided lubrication for areas not lubricated by oil.

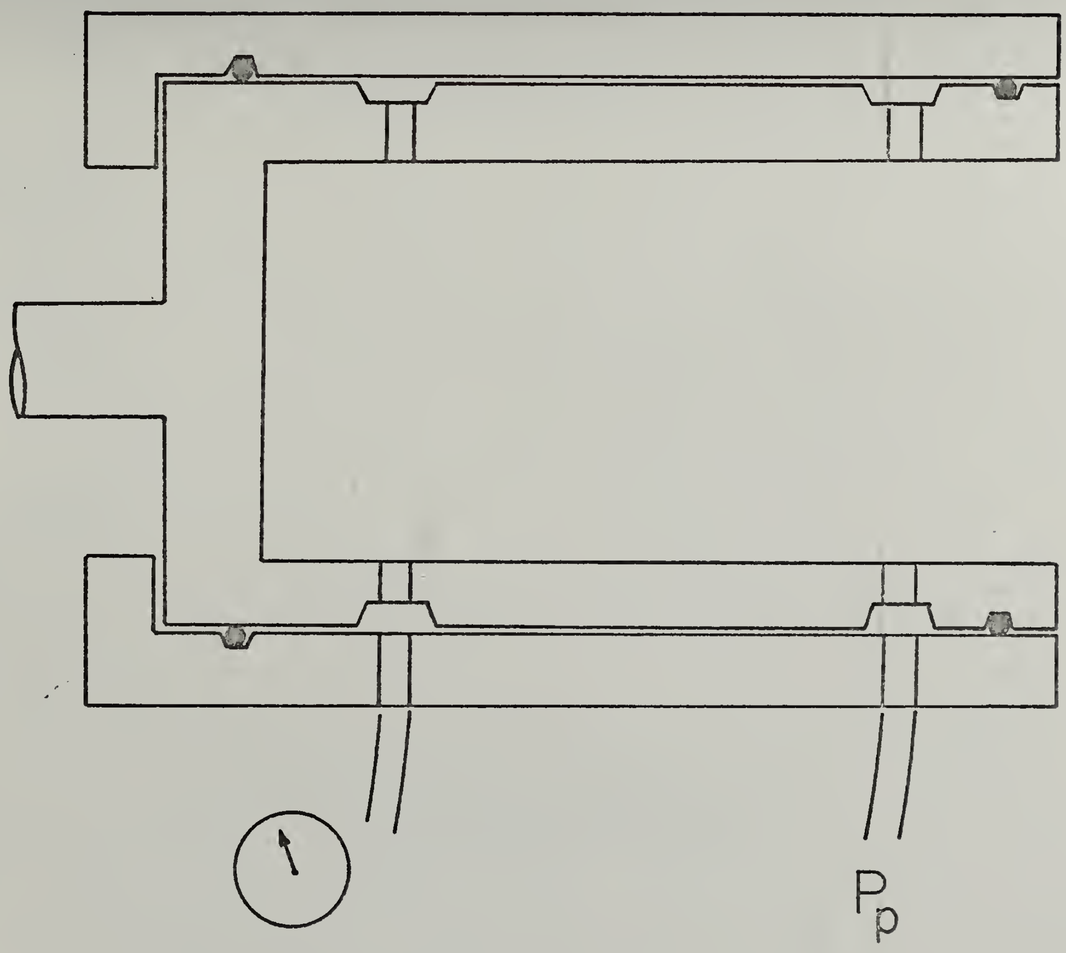

Figure 10
Position of O-ring Seals

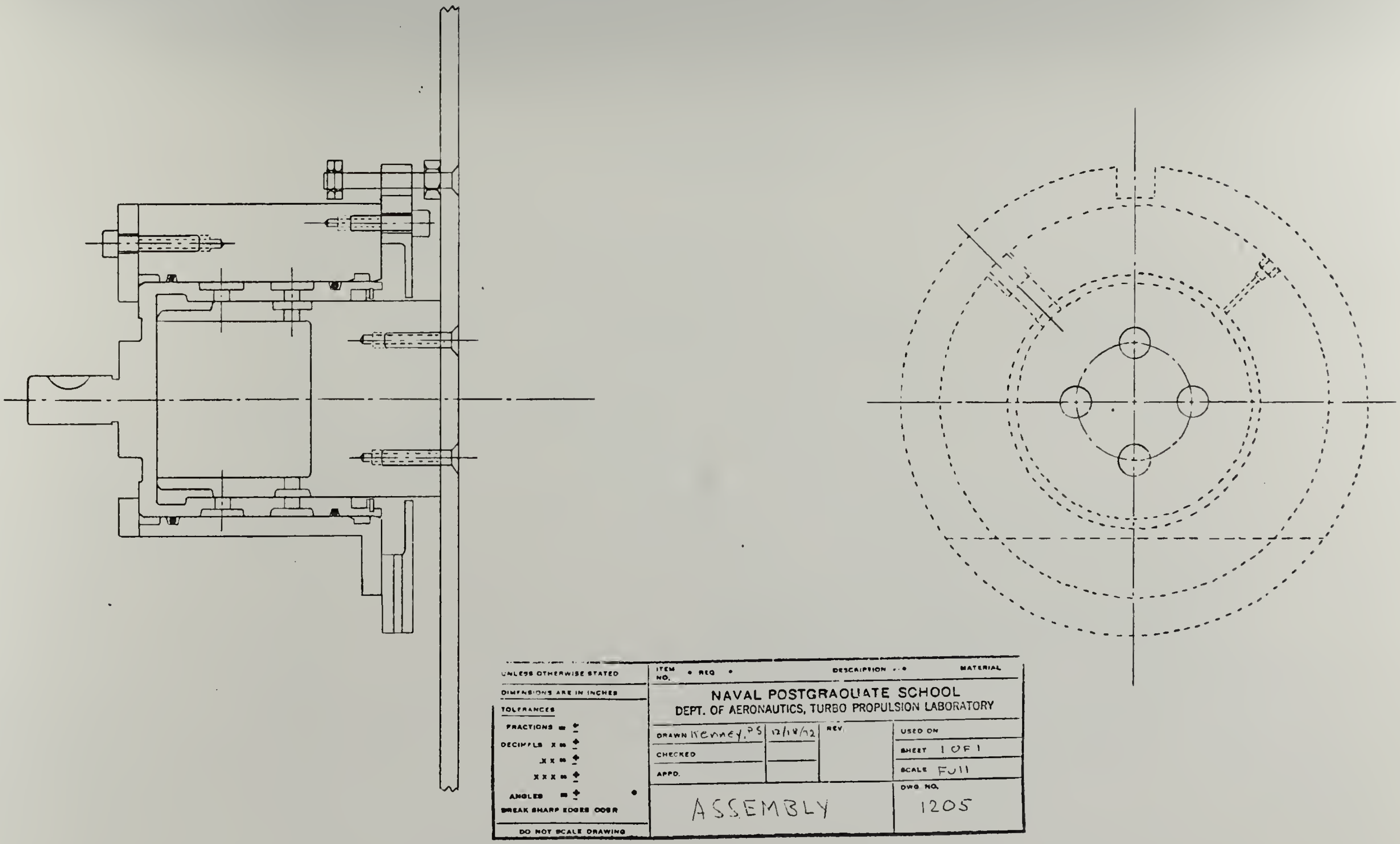

Figure 11
Assembly Drawing

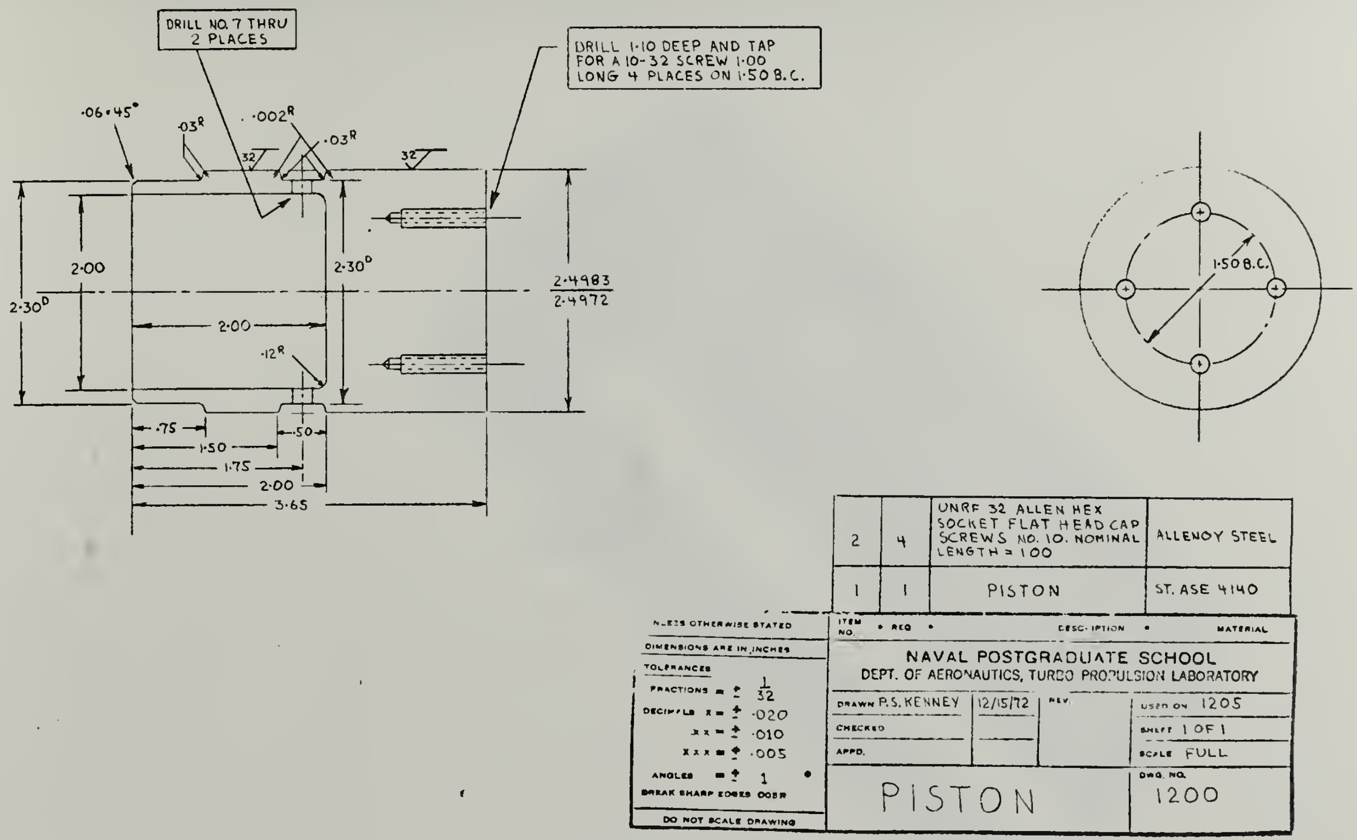

Figure 12A
Piston Drawing

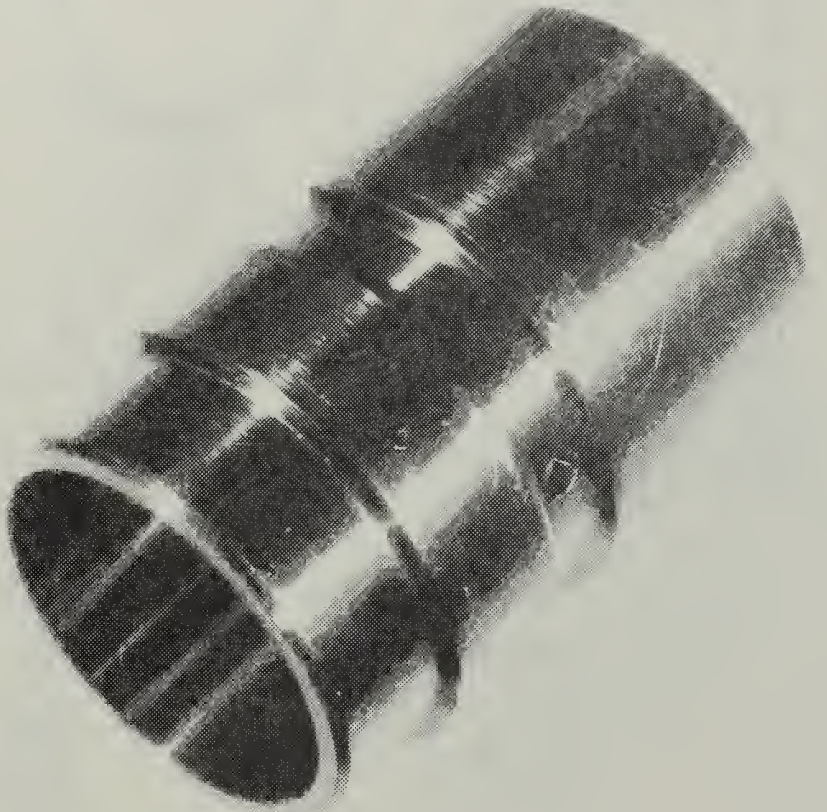

Figure 12B
Piston Photograph

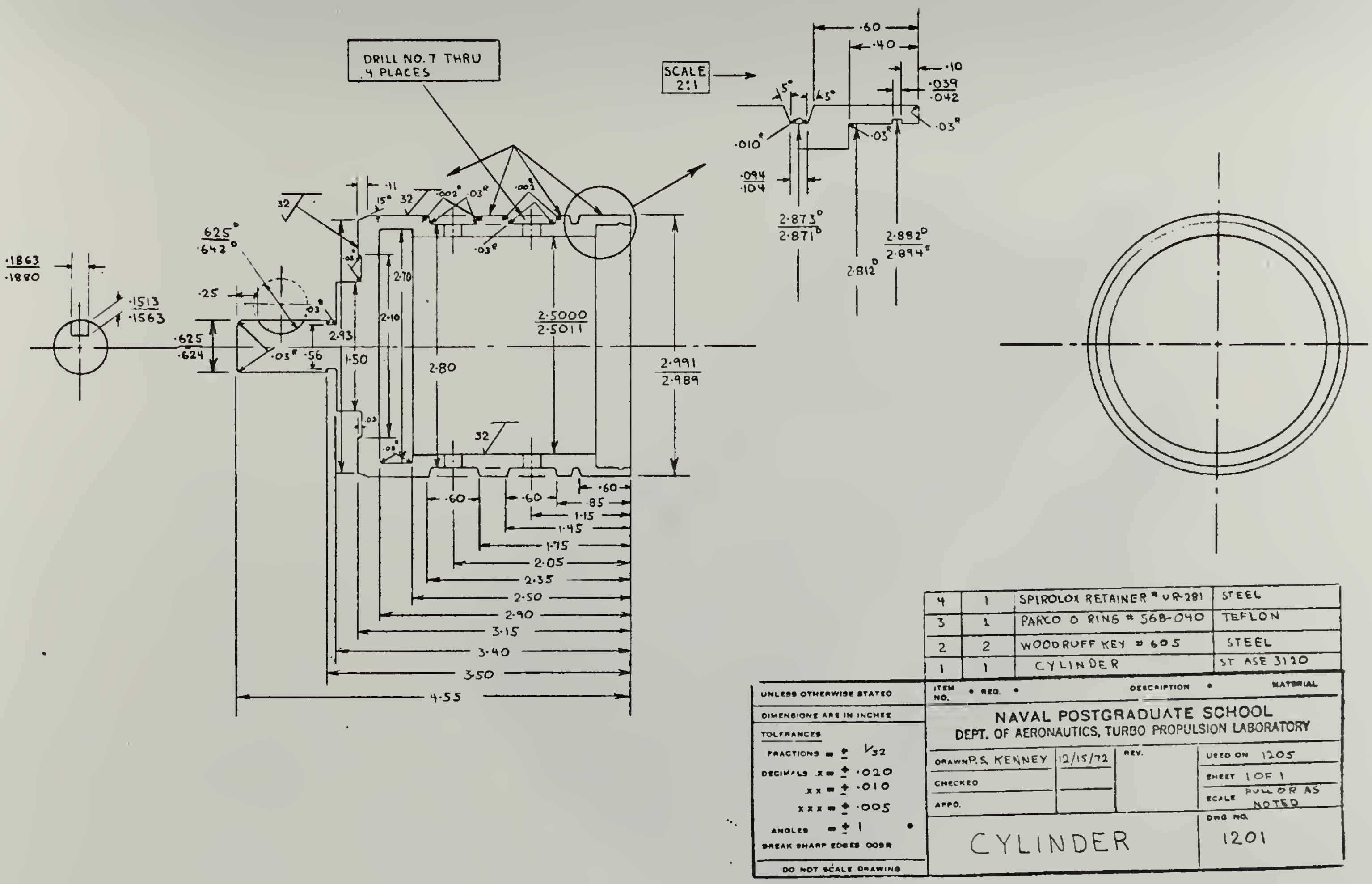

Figure 13A

Cylinder Drawing

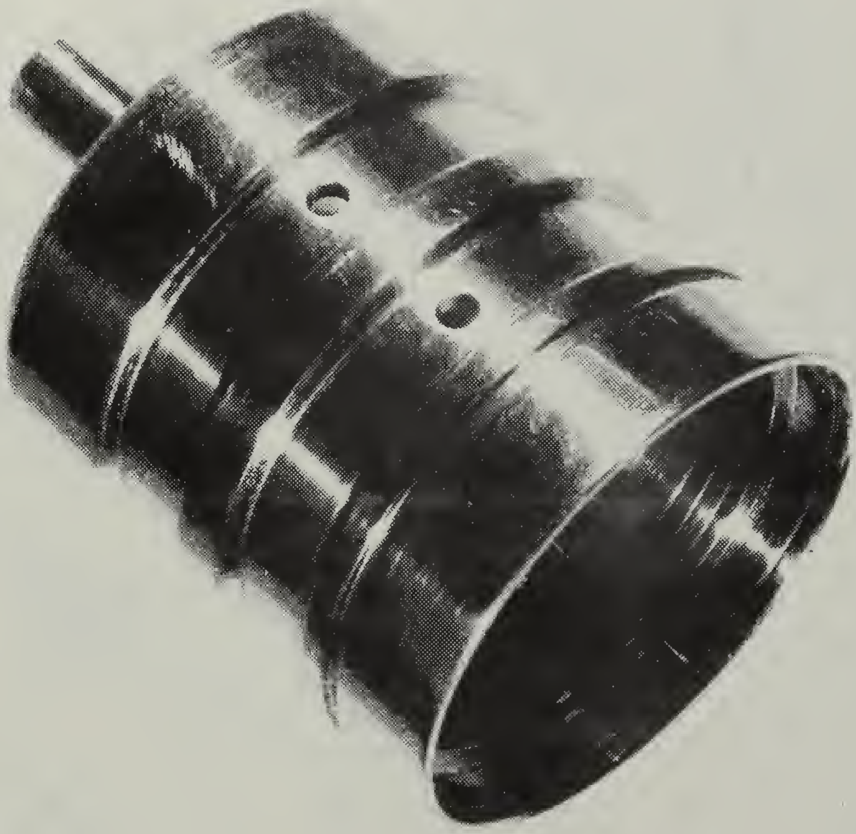

Figure 13B
Cylinder Photograph

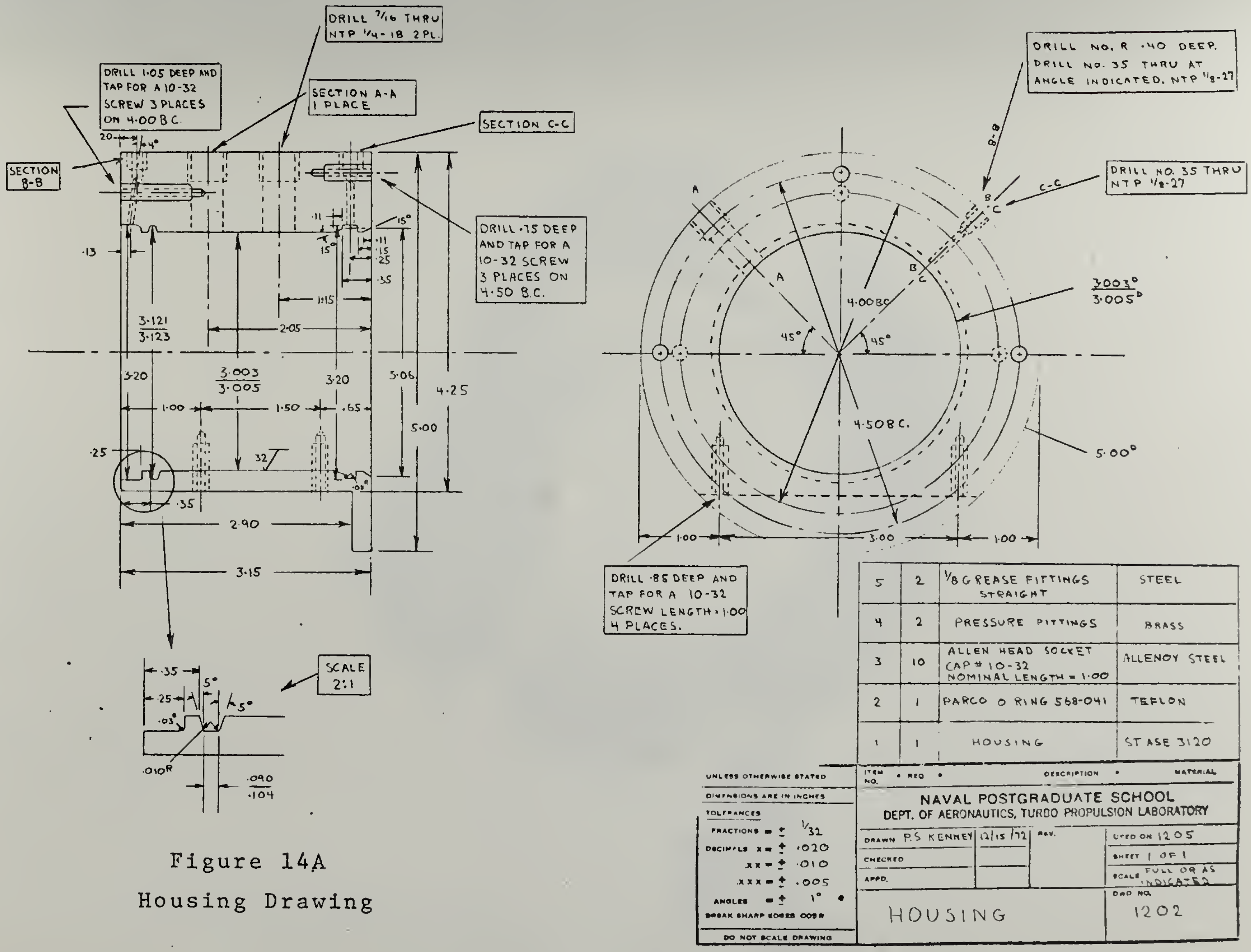

ITEM NO.	REQ	DESCRIPTION	MATERIAL
5	2	1/8 GREASE FITTINGS STRAIGHT	STEEL
4	2	PRESSURE PITTINGS	BRASS
3	10	ALLEN HEAD SOCKET CAP # 10-32 NOMINAL LENGTH = 1·00	ALLENOY STEEL
2	1	PARCO O RING 568-041	TEFLON
1	1	HOUSING	ST ASE 3120

UNLESS OTHERWISE STATED
DIMENSIONS ARE IN INCHES
TOLERANCES
FRACTIONS = ± 1/32
DECIMALS .X = ± ·020
.XX = ± ·010
.XXX = ± ·005
ANGLES = ± 1°
BREAK SHARP EDGES ·005 R
DO NOT SCALE DRAWING

NAVAL POSTGRADUATE SCHOOL
DEPT. OF AERONAUTICS, TURBO PROPULSION LABORATORY

DRAWN P.S KENNEY	12/15/72	REV.
CHECKED		
APPD.		

USED ON 1205
SHEET 1 OF 1
SCALE FULL OR AS INDICATED
DWG NO. 1202

HOUSING

Figure 14A

Housing Drawing

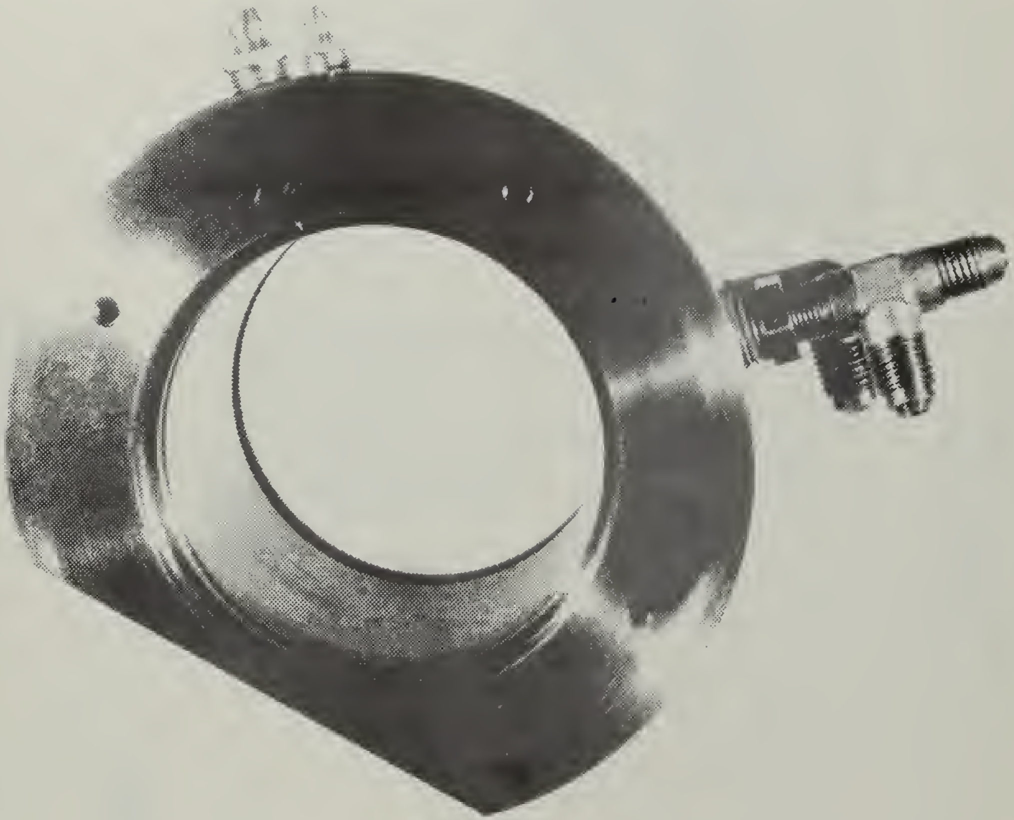

Figure 14B
Housing Photograph

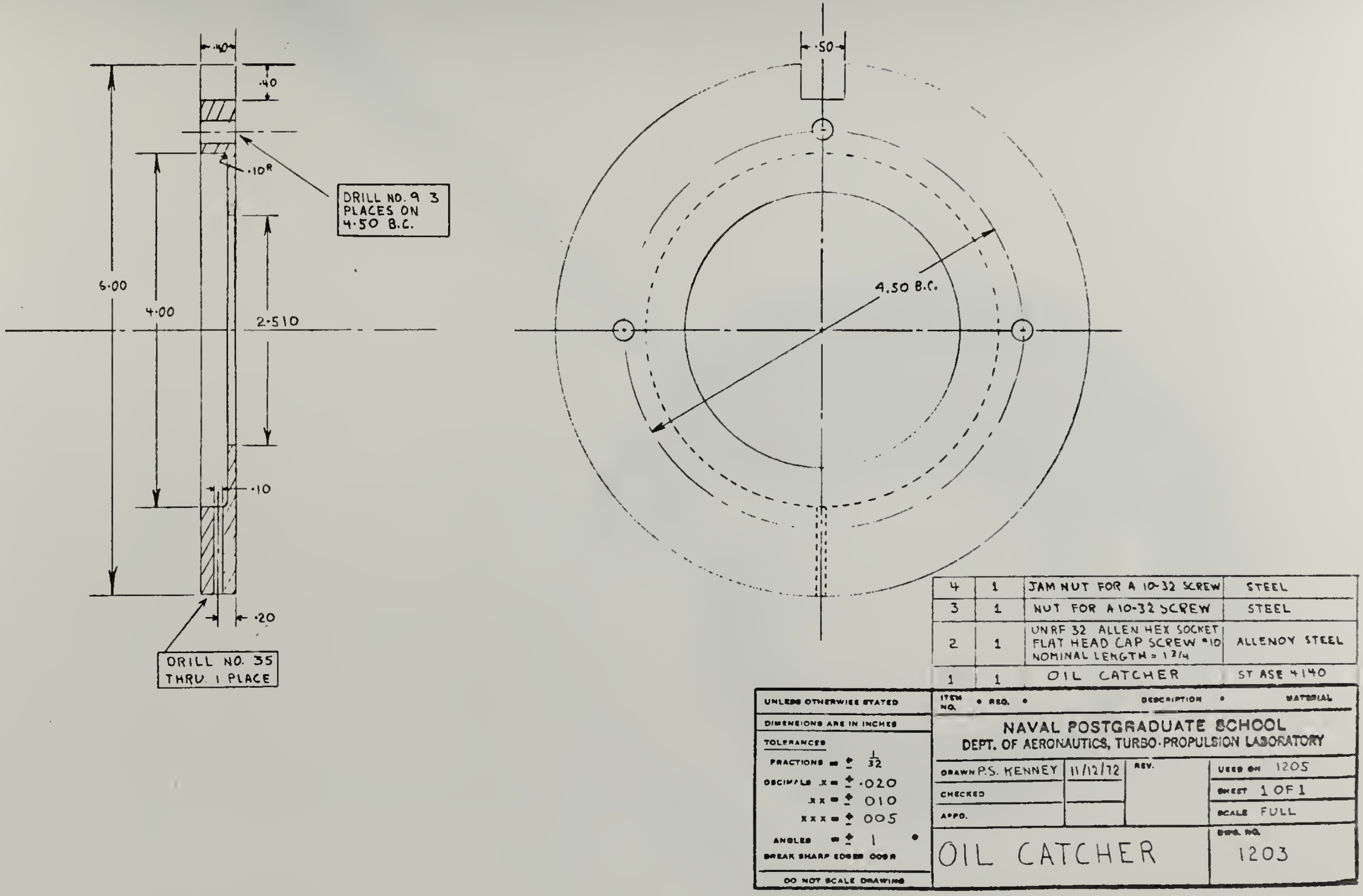

Figure 15A
Oil Catcher Drawing

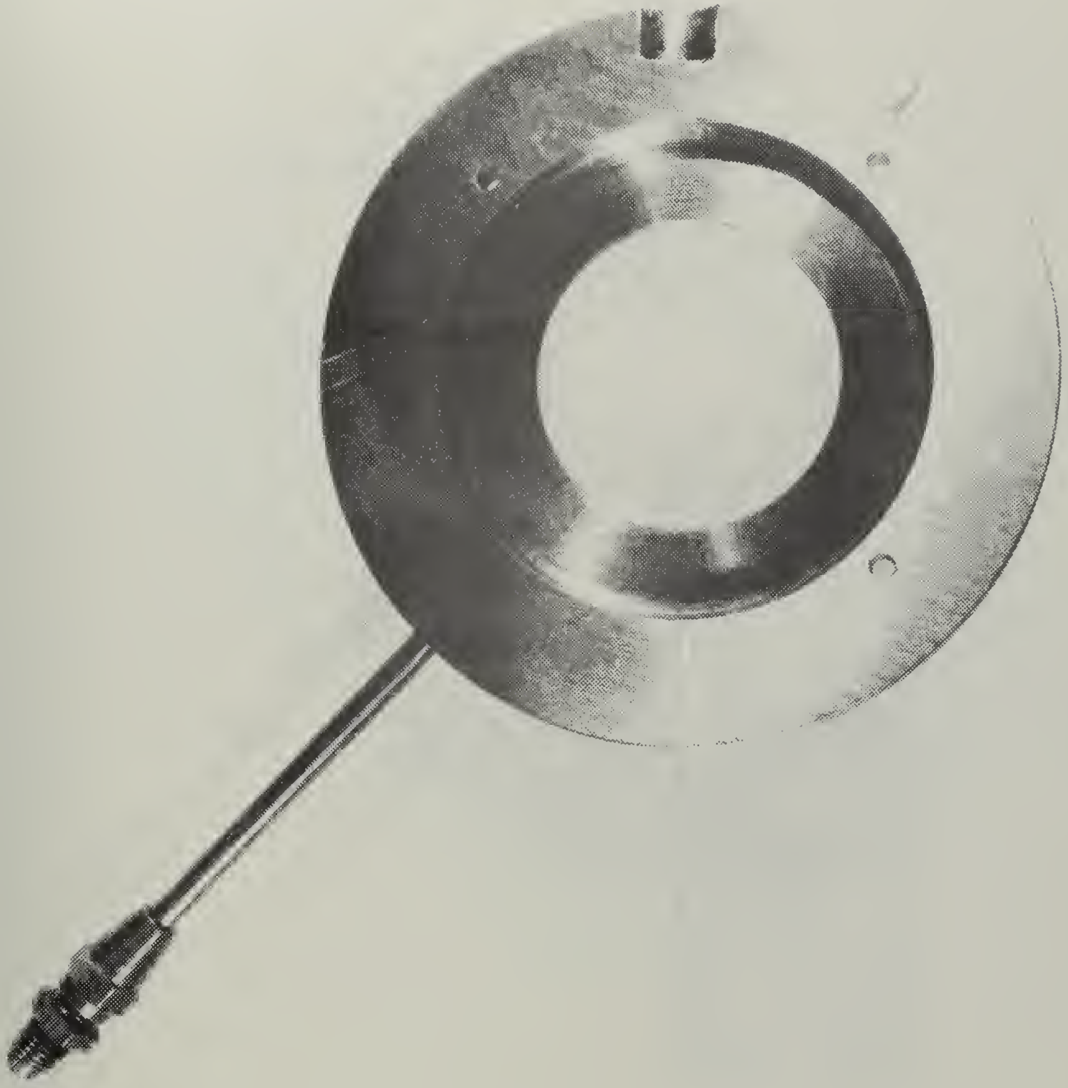

Figure 15B
Oil Catcher Photograph

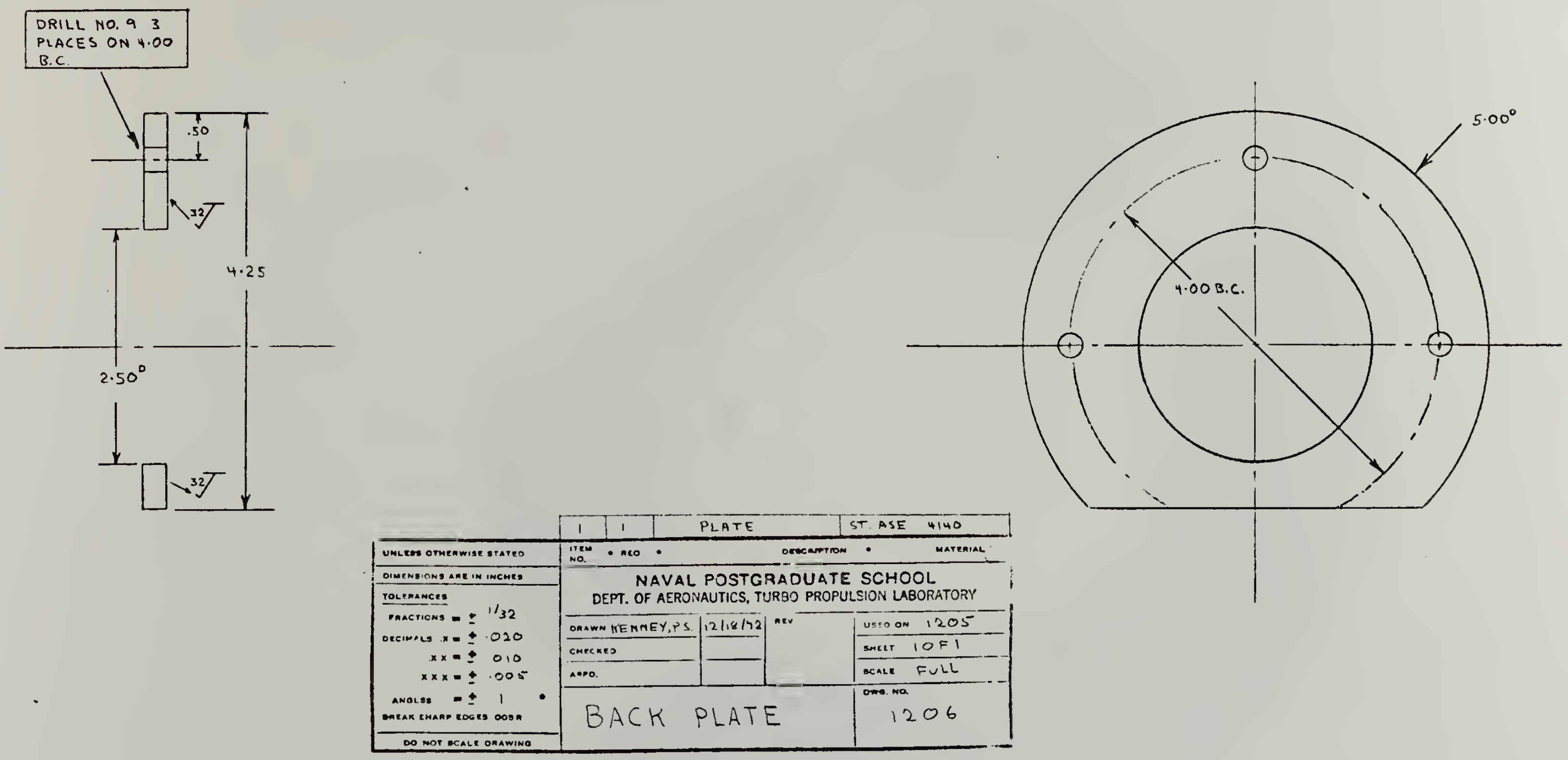

Figure 16A

Back Plate Drawing

Figure 16B
Back Plate Photograph

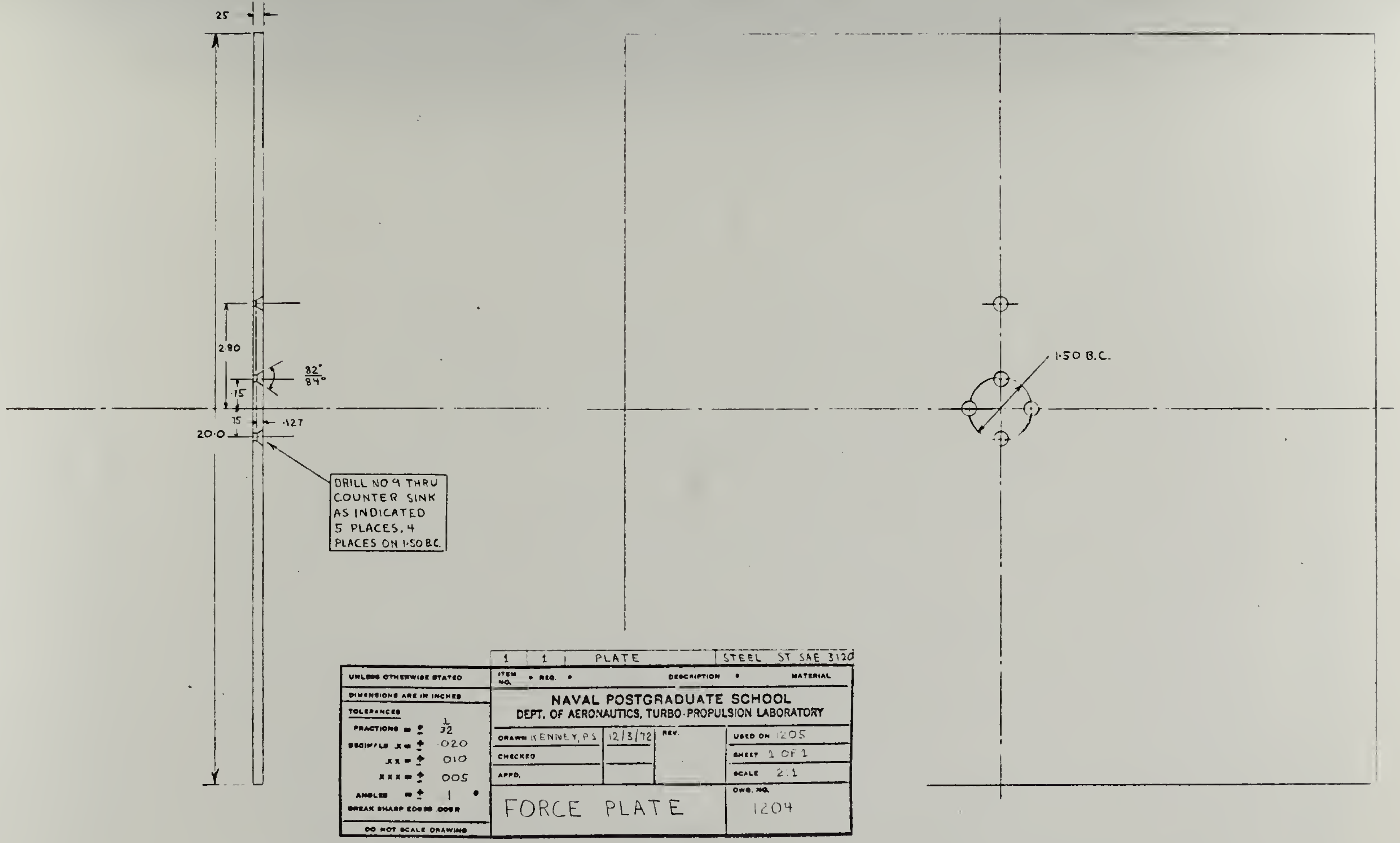

Figure 17

Force Plate Drawing

IV. EXPERIMENTAL APPARATUS, PROCEDURES, AND RESULTS

The experimental set-up is shown in Figure 18. Air supplied by the Allis-Chalmers twelve-stage axial compressor passed through a control valve and into a settling tank. The flow then passed through a standard ASME sharp edge orifice into a second tank. From this tank, the flow passed through an eight-inch diameter pipe into a transition piece which changed the cross section to a five-inch square area. From this point, the flow passed through a honeycomb flow straightener and into the model. Figure 18 shows the straight channel model configuration. All channels of different turning angles had a centerline radius of 12.5 inches and were attached at the connection point. The flow rate was controlled by the valve and determined from measurements taken with two slant tube mercury manometers combined with a total temperature measurement at the orifice. Total pressure and temperature were measured in the eight-inch diameter pipe. All pressures measured between the second settling tank and the model exit were made with water U-tube manometers. The mercury manometers had an accuracy of ± .005 inches of mercury. U-tube manometers had an accuracy of ± .05 inches of water.

A. PROBE SURVEYS

The first set of experiments consisted of Prandtl probe surveys at the discharge of a 19.5 inch long straight

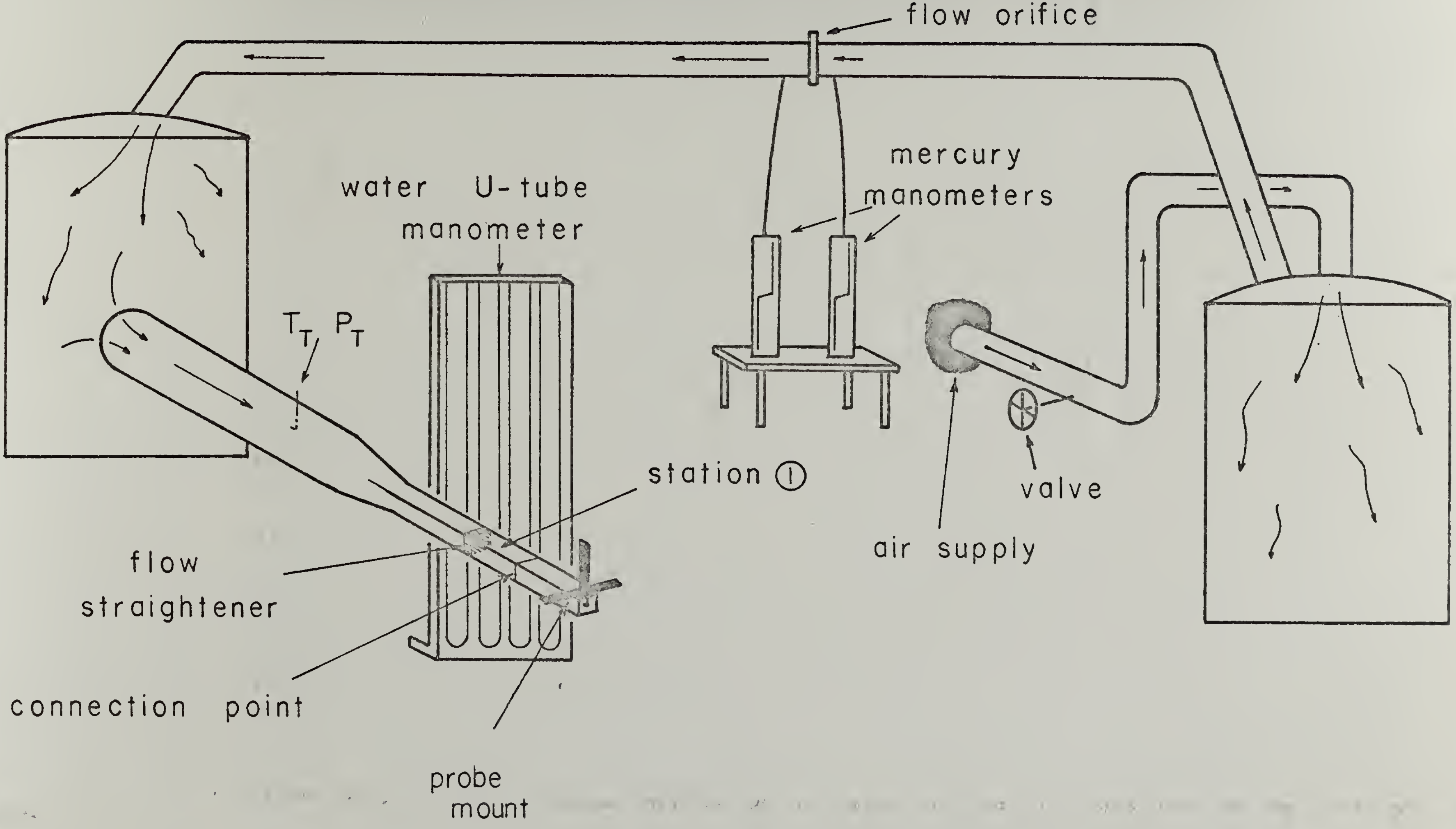

Figure 18

Experimental Set-Up

channel to investigate the velocity profile and to determine the mass flow rate. All channel lengths were measured from the connection point to the exit along the channel centerline. With the exception of regions near the wall and in the corners, the velocity profile was nearly uniform as shown in Figure 19. The mass flow obtained by numerical integration of the probe measurements over the channel exit agreed with the orifice measurement within 1.5 percent.

The second set of experiments were performed with a 90° bend approximately 20 inches long. The purpose of these experiments was to investigate the flow field existing at the bend discharge. Yaw angles were determined with a Cobra probe and are shown in Figure 20. The arrows represent the angular deflection of the flow with respect to a plane perpendicular to the exit plane. Survey points along the lower wall are absent because of probe vibrations. The probe was reinforced to prevent this problem in later experiments. The results showed an overall angular deflection in the x-direction. This indicated that the flow was not turned by 90° but was following the path shown in Figure 21. As a result, secondary flow vortices were imposed upon the average angle θ. To eliminate this condition, a straight section 10 inches in length was attached to the discharge of the 90° bend.

The third set of experiments was carried out with this arrangement. Yaw and pitch angles were determined with a Cobra probe mounted in the horizontal and vertical positions. The results are shown in Figures 22 and 23. The arrows

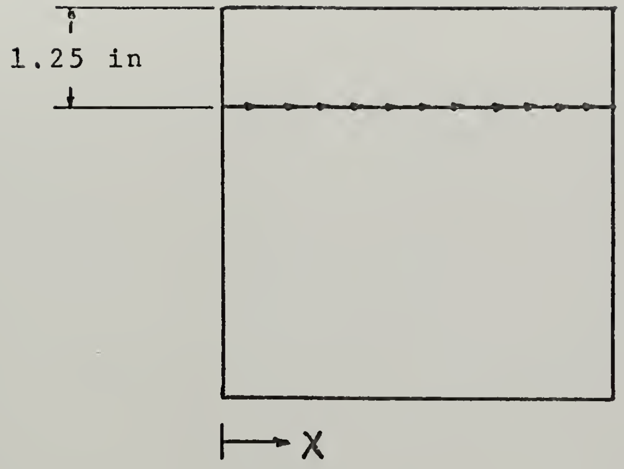

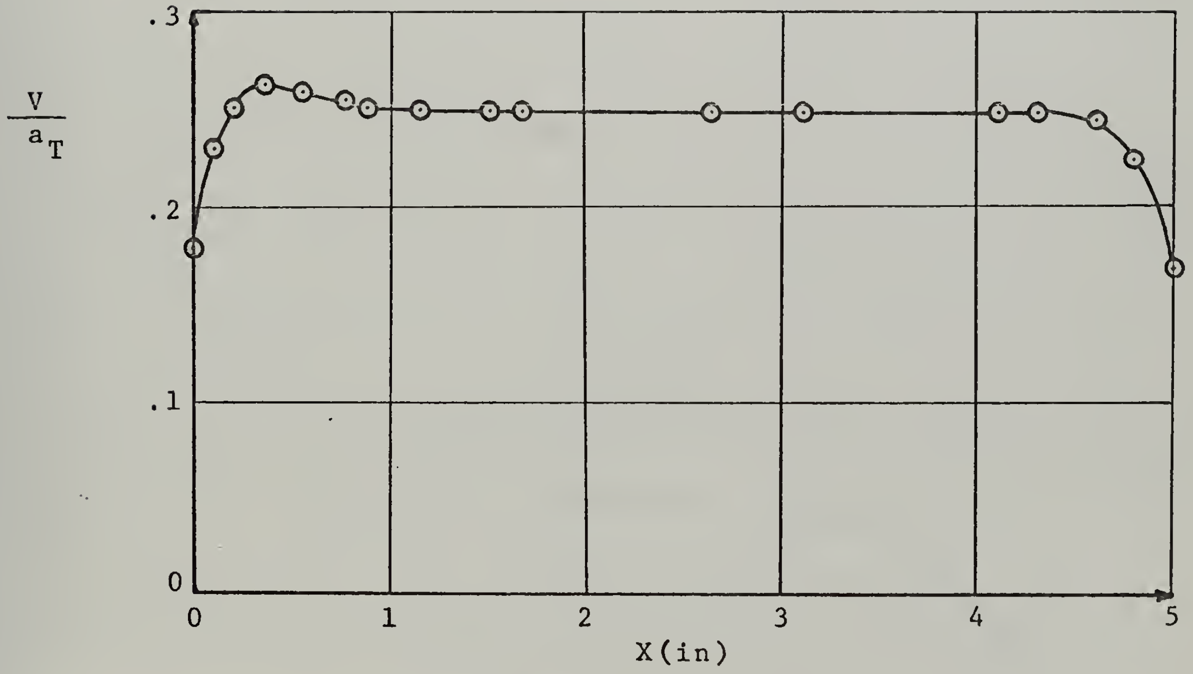

Exit velocity divided by the total speed of sound "V/a_T" as a function of distance "X."

Figure 19

Prandtl Probe Survey of the Straight Channel

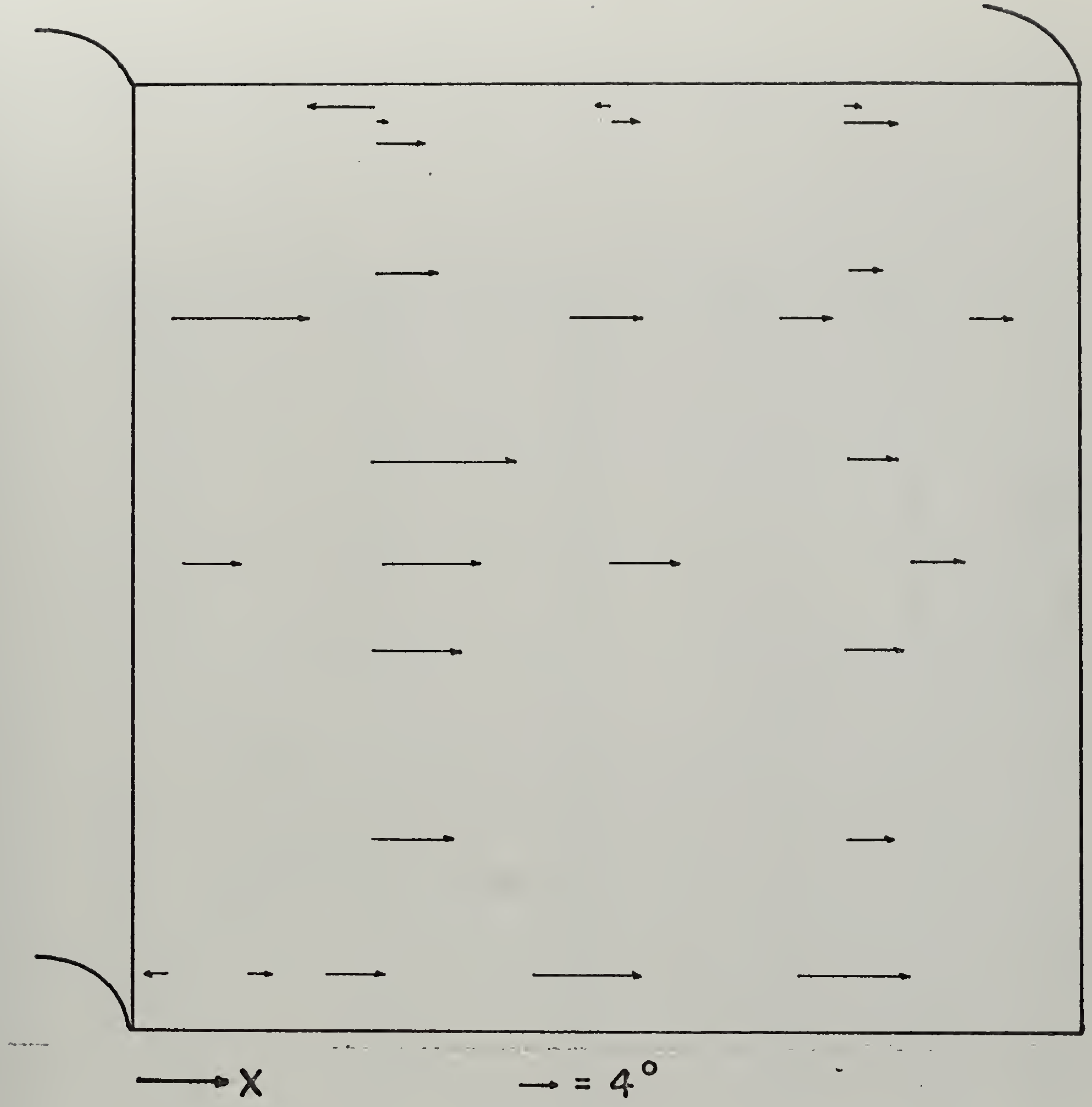

Figure 20
Yaw Angles in the 90 Degree Bend

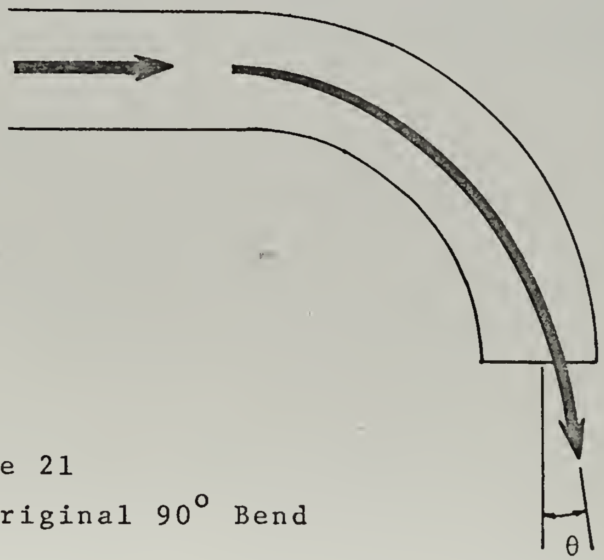

Figure 21
Flow Path for Original 90° Bend

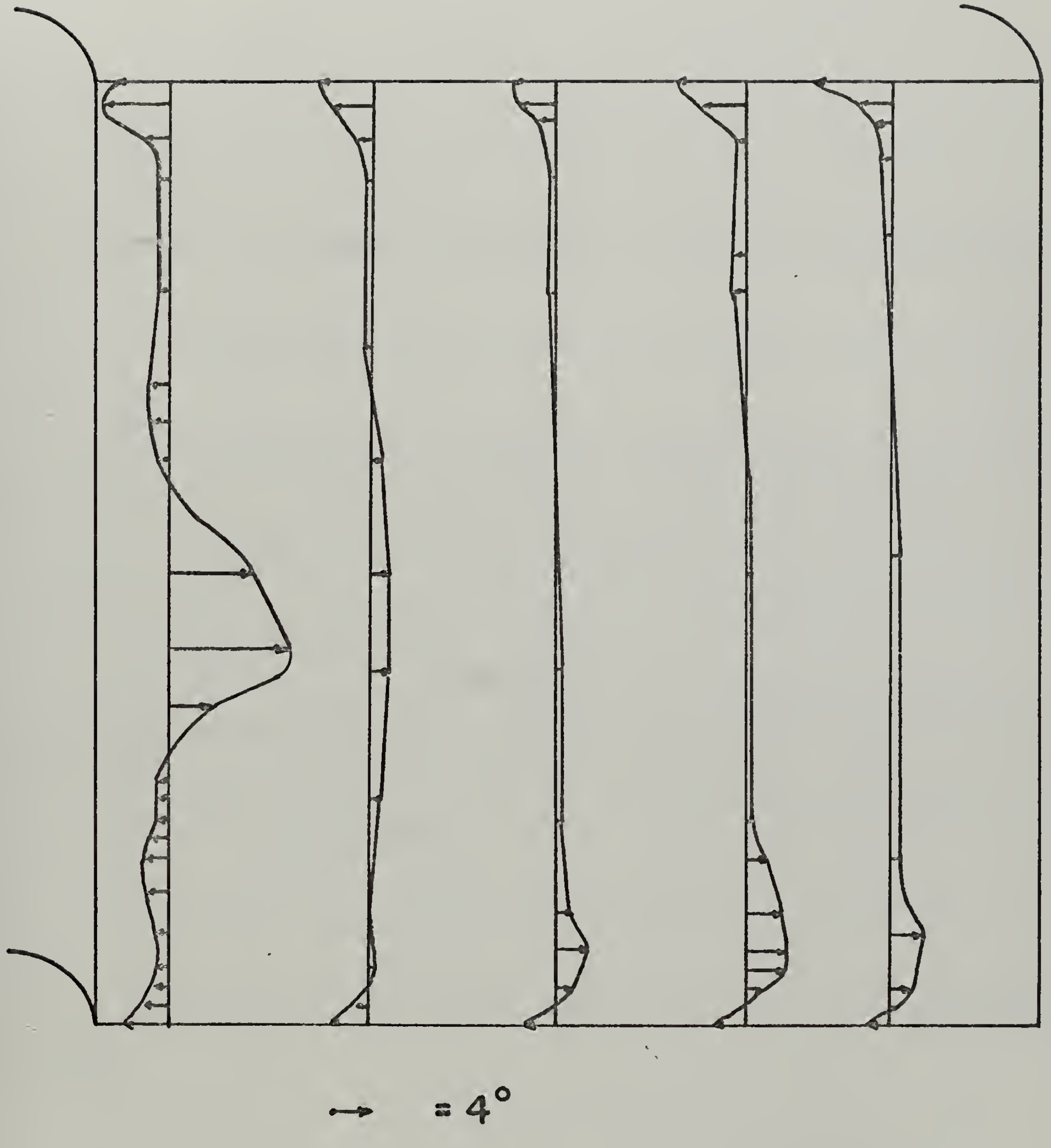

Figure 22

Yaw Angles Induced by Secondary Flow in the 90 Degree Bend

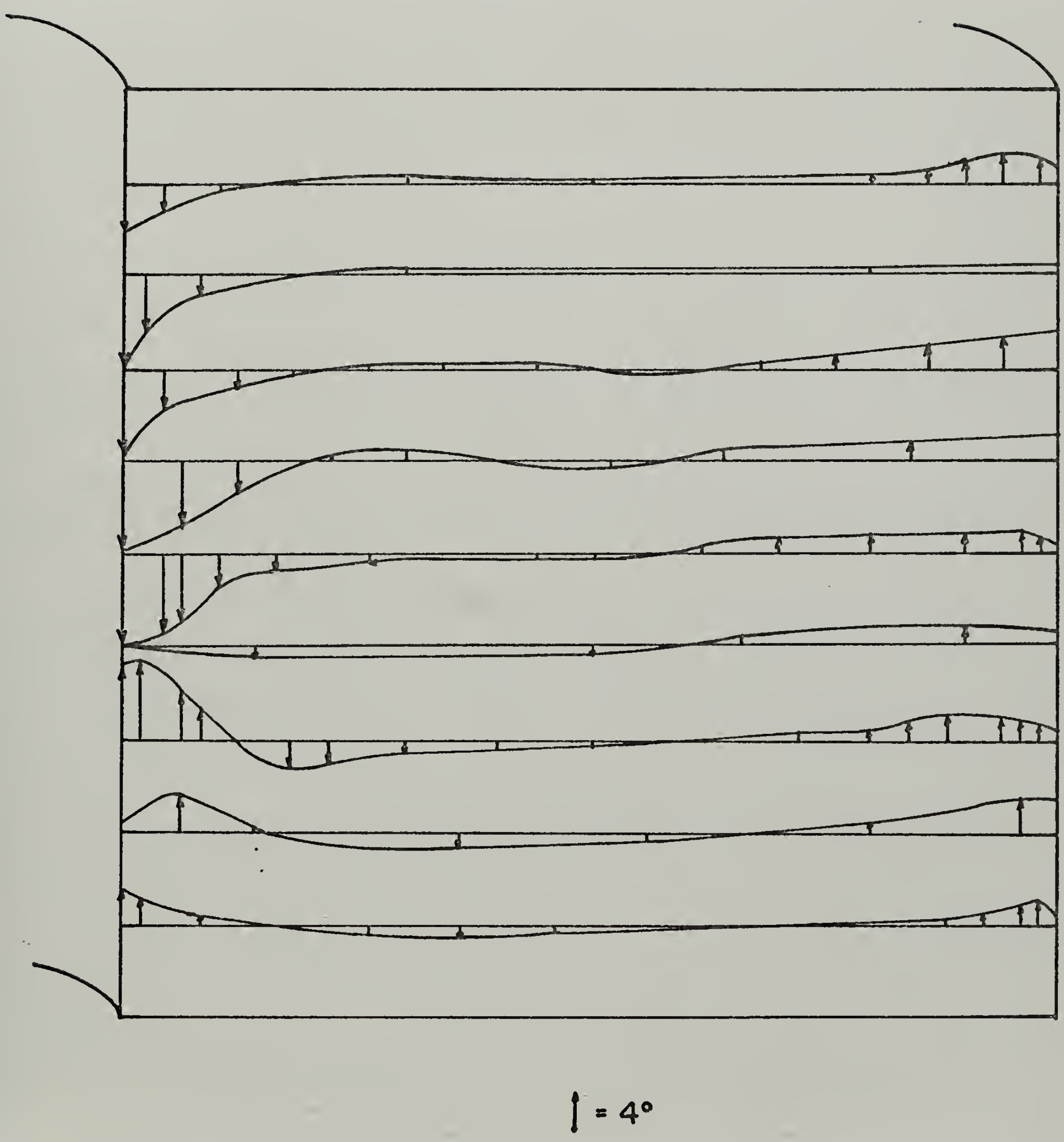

Figure 23
Pitch Angles Induced by Secondary Flow in the 90 Degree Bend

represent flow angles measured with respect to a plane perpendicular to the exit plane. From these results, the angle θ of Figure 21 appears to be equal to zero.

The same arrangement was used for the final set of surveys which were taken with a Kiel probe. The purpose of these experiments was to determine the total pressure loss distribution over the exit plane. The loss is represented by the factor

$$\chi = \frac{P_T - P_{TK}}{P_T}$$

where P_T = reference total pressure measured by a Kiel probe in the eight-inch diameter pipe.

P_{TK} = total pressure measured by the survey Kiel probe at the model exit.

The magnitude of χ does not represent total pressure loss caused by secondary flow. Losses that occur between the reference Kiel probe and the connection point are also included in χ along with secondary losses from the connection point to the channel exit. Values of χ are only important in showing the distribution of the losses over the exit plane. The results are shown in Figure 24. The curves represent contours of constant loss.

B. FORCE PLATE MEASUREMENTS

The hydraulic force plate apparatus designed for this study was not used. Problems encountered with the apparatus are discussed in Appendix B. The force plate system that

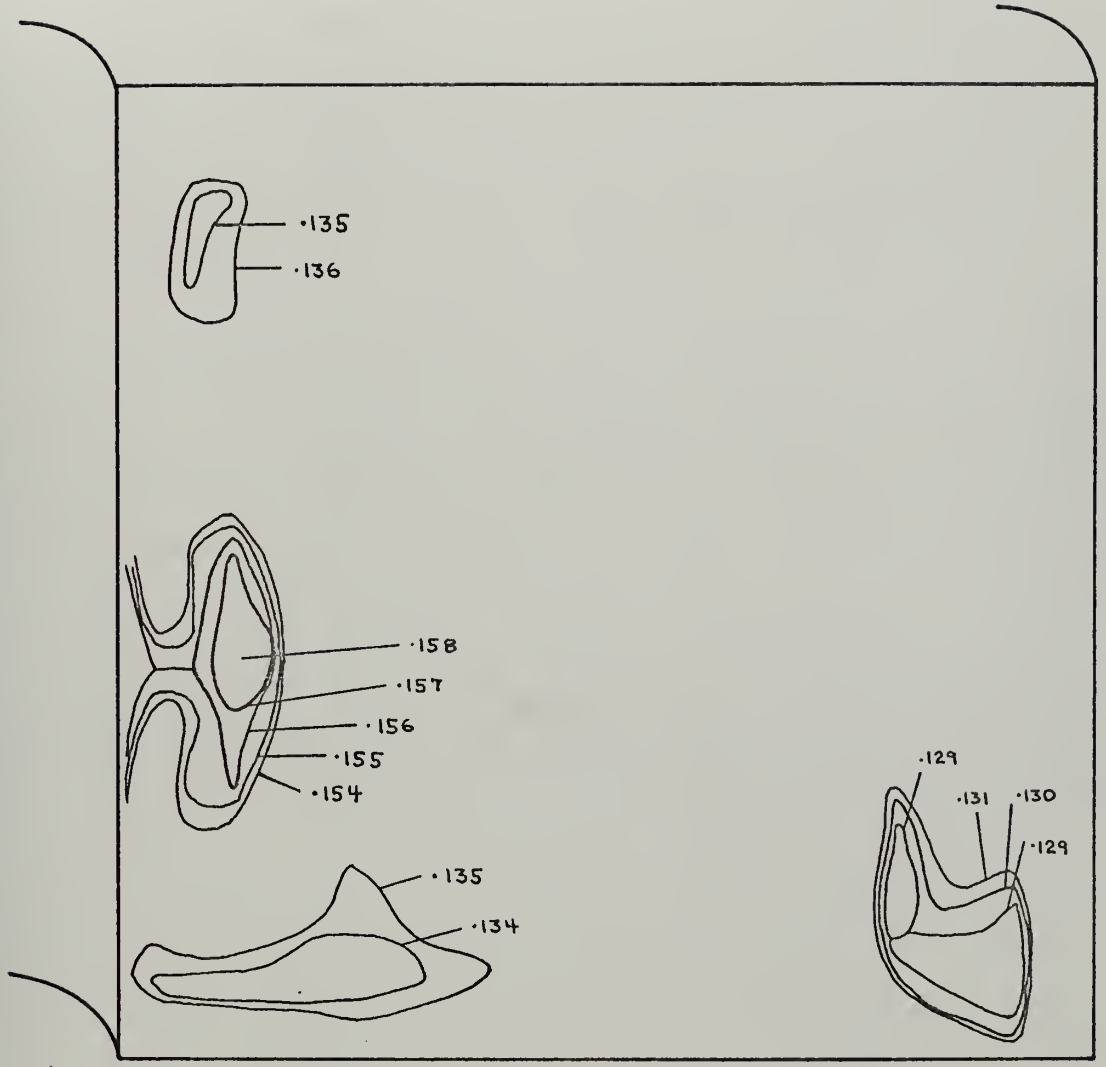

Contours of constant total pressure loss with "χ" indicated.

Figure 24

Total Pressure Loss Distribution for the 90 Degree Bend

was used is shown in Figure 25. The force on the plate was transmitted to a variable reluctance force transducer by a steel shaft supported by axially sliding ball bearings. The force transducer was loaded in tension and calibrated to display force in pounds and tenths of pounds on the counter. Adjusting bolts were used to adjust the height and pitch of the plate. The maximum system error was ± 0.2 pounds.

Experiments were conducted with channels of 0°, 45°, 90° and 135° of turning. All channels were approximately thirty inches in length and the last ten inches of each channel consisted of a straight section. Investigation of the flow at the discharge indicated that the overall flow path was perpendicular to the exit plane. The force plate was positioned thirteen inches from the exit plane and parallel to it. Loss coefficients were determined as described in Appendix A. The loss coefficients are tabulated in Table I and plotted against Reynolds number in Figures 26 - 29 with the Mach number for each point indicated. $\overline{\zeta}$ is the average total loss coefficient for a particular channel. Average secondary flow loss coefficients ($\overline{\zeta}_s$) for the curved channels were taken as the difference between the average total loss coefficient for each bend and the average total loss coefficient for the straight channel. Hence,

$$\overline{\zeta}_s\ (45^\circ) = 0.0166$$

$$\overline{\zeta}_s\ (90^\circ) = 0.0317$$

$$\overline{\zeta}_s\ (135^\circ) = 0.0722$$

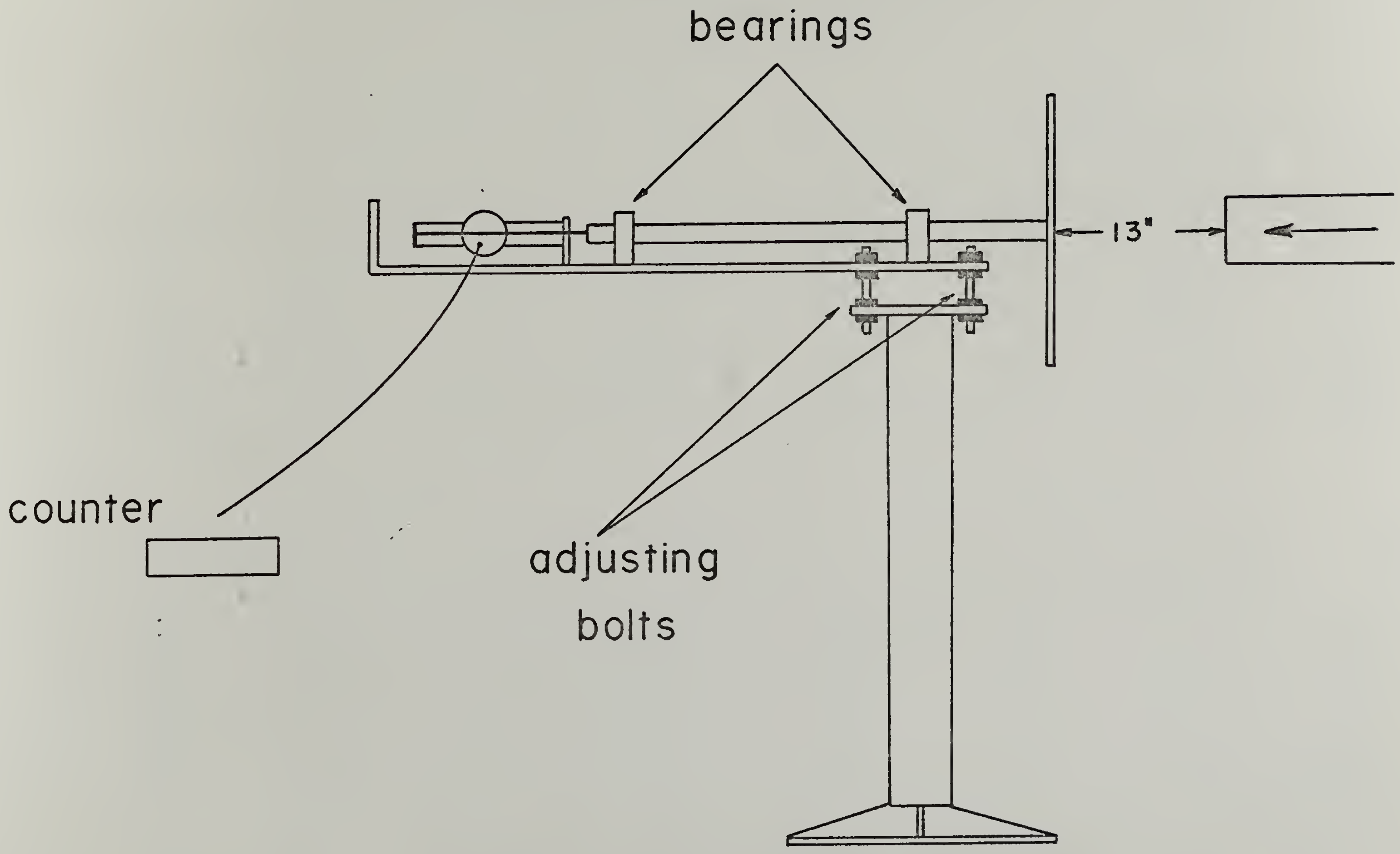

Figure 25
Force Plate Apparatus

TABLE I

LOSS COEFFICIENTS

Straight Channel

M	Re x 10^{-5}	$\dot{m}$ lbm/sec	ζ
.1974	5.374	2.823	.0101
.2207	5.985	3.151	.0103
.2371	6.411	3.381	.0118
.2574	6.951	3.669	.0186
.2712	7.322	3.866	.0287
.2879	7.768	4.103	.0255
.3058	8.249	4.358	.0331

45° Bend

M	Re x 10^{-5}	$\dot{m}$ lbm/sec	ζ
.1966	5.409	2.837	.0257
.2143	5.763	3.064	.0363
.2360	6.478	3.402	.0324
.2548	6.896	3.653	.0374
.2789	7.659	4.021	.0392
.2923	7.693	4.201	.0398
.3107	8.518	4.477	.0438

90° Bend

M	Re x 10^{-5}	$\dot{m}$ lbm/sec	ζ
.2060	5.553	2.934	.0457
.2182	5.824	3.096	.0623
.2352	6.341	3.350	.0440
.2530	6.777	3.595	.0568
.2779	7.504	3.961	.0489
.2858	7.698	4.070	.0519
.3048	8.242	4.347	.0509

135° Bend

M	Re x 10^{-5}	$\dot{m}$ lbm/sec	ζ
.1962	5.355	2.815	.0926
.2208	5.926	3.147	.0970
.2439	6.646	3.497	.0916
.2568	6.926	3.667	.0961
.2707	7.371	3.880	.0916
.2844	7.713	4.070	.0881
.3110	8.507	4.471	.0868

$\bar{\zeta}$ (0) = .0198 $\bar{\zeta}$ (45) = .0364 $\bar{\zeta}$ (90) = .0515 $\bar{\zeta}$ (135) = .0920

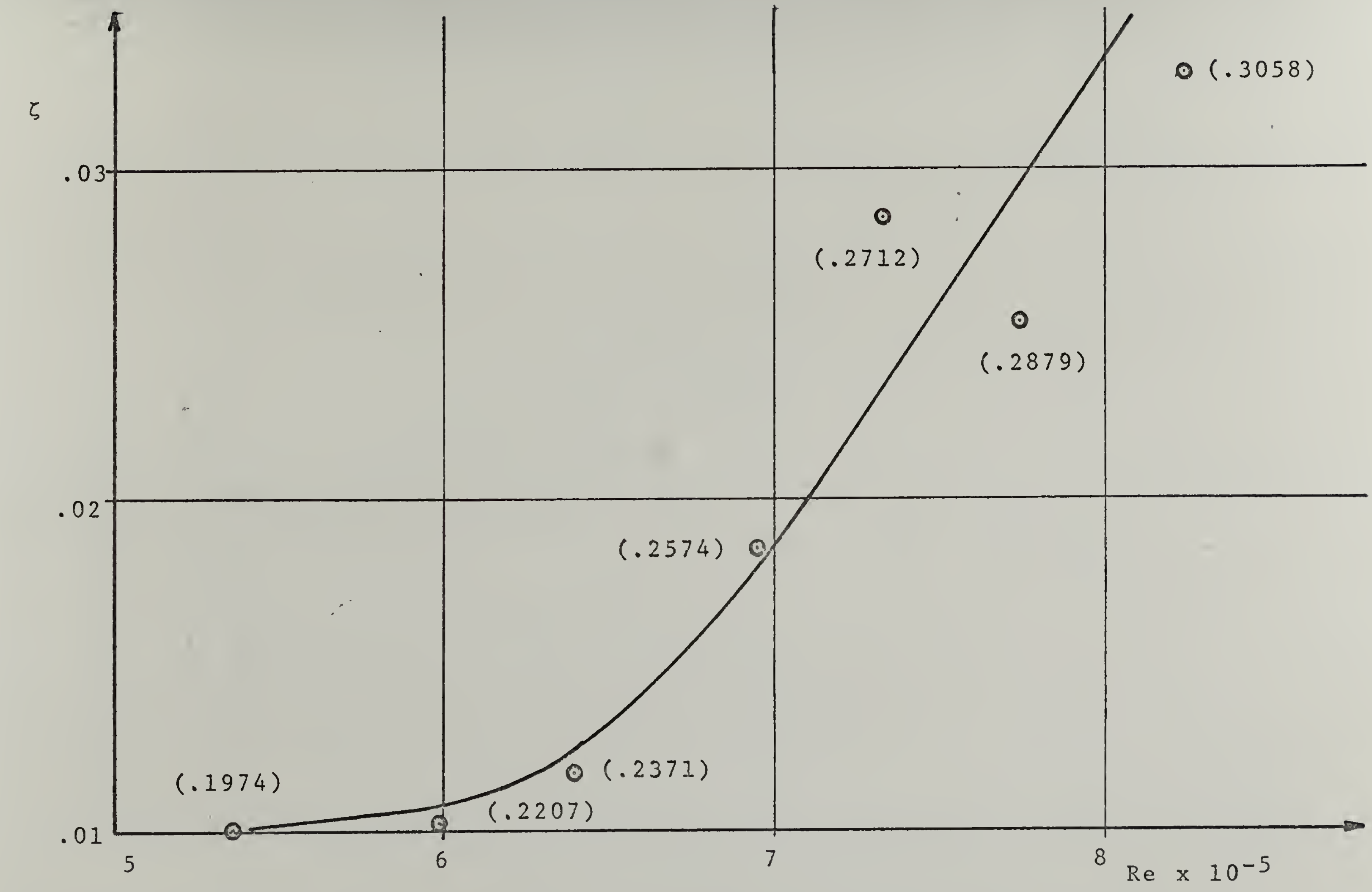

Loss coefficient "ζ" as a function of Reynolds number "Re" with Mach number "( )" indicated.

Figure 26
Loss Coefficients for the Straight Channel

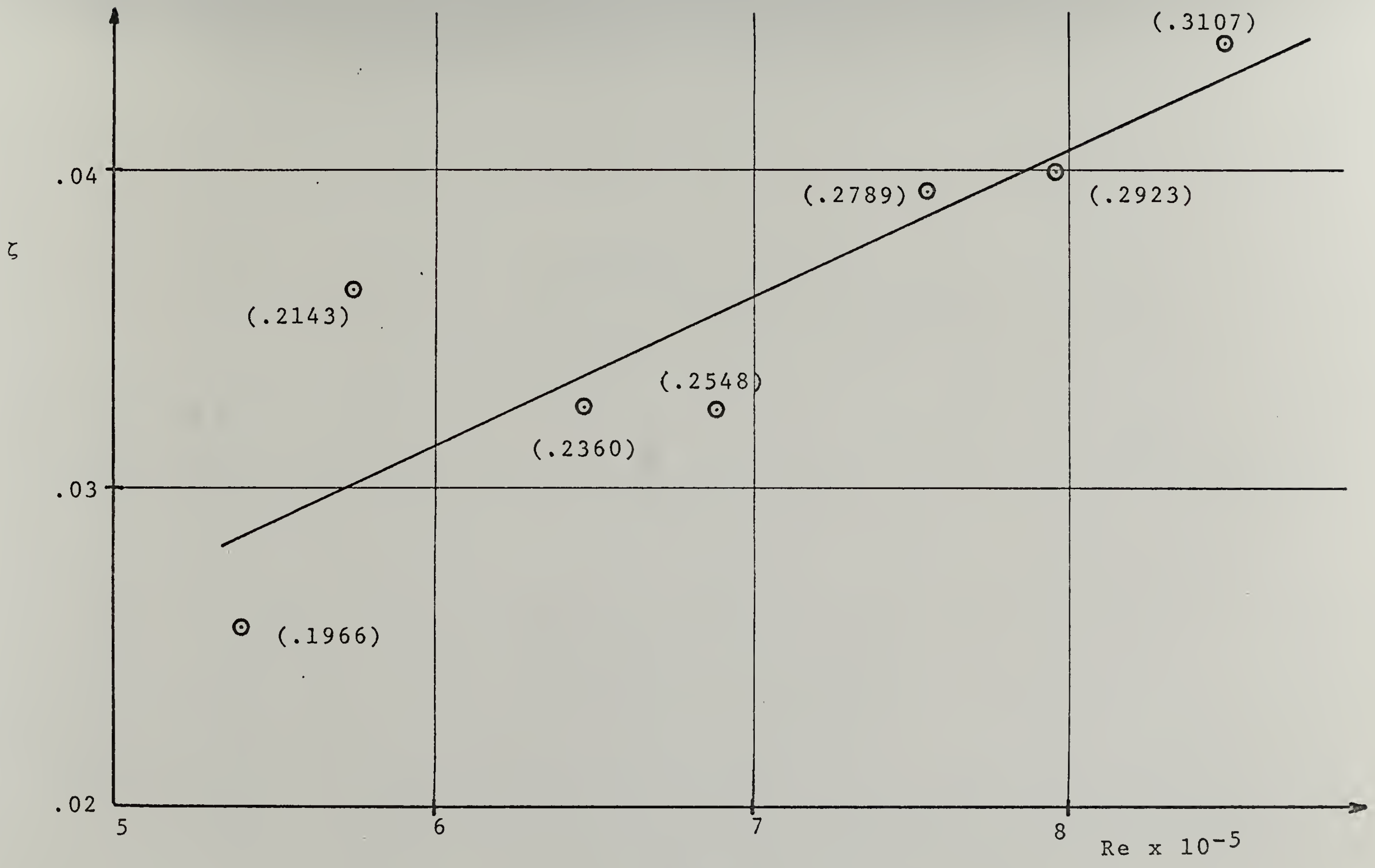

Figure 27

Loss Coefficients for the 45 Degree Bend

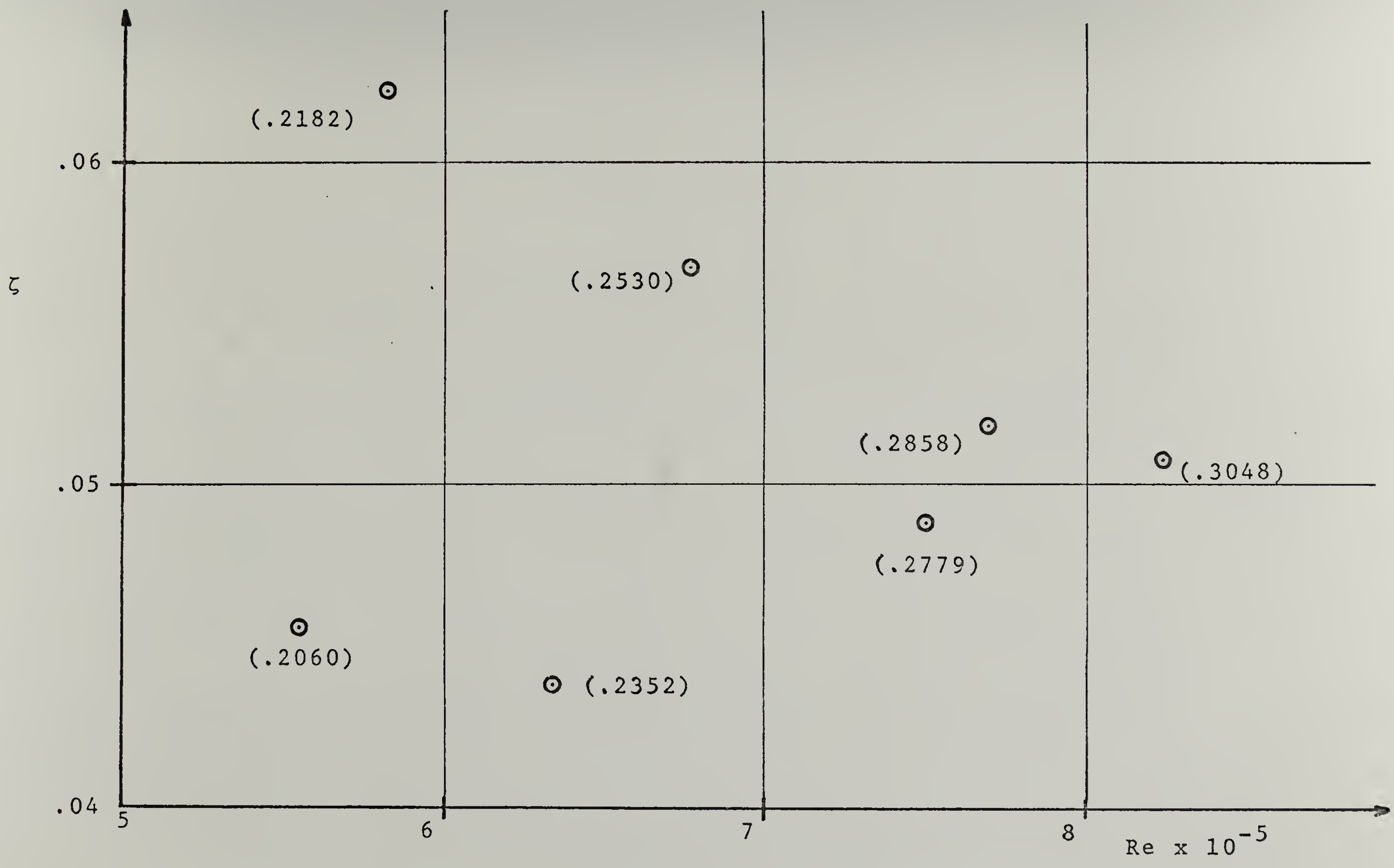

Figure 28

Loss Coefficients for the 90 Degree Bend

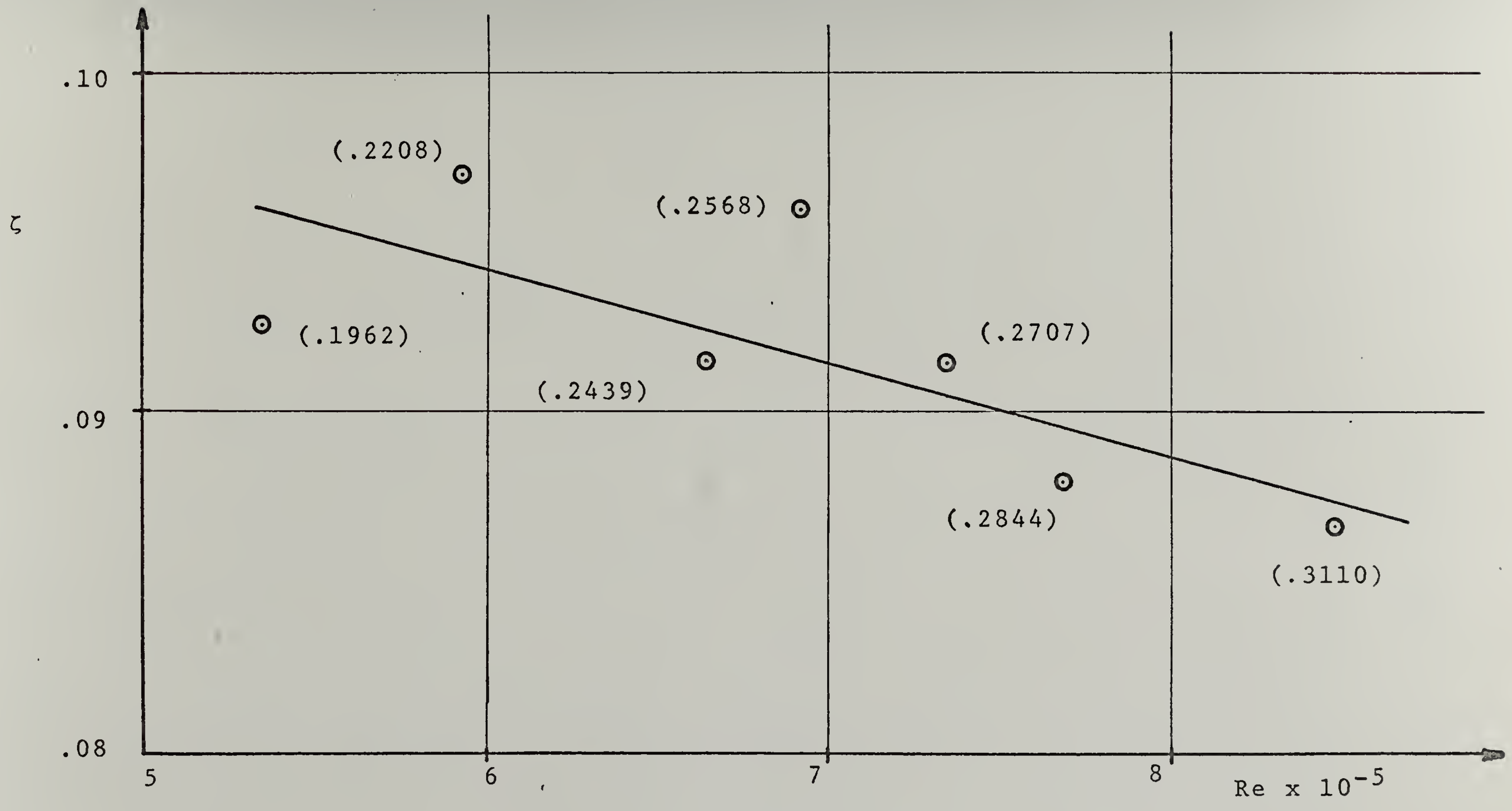

Figure 29

Loss Coefficients for the 135 Degree Bend

V. CONCLUSIONS

The force plate was extremely valuable in determining the actual momentum of the flow. The measurements were very successful in determining average loss coefficients. As shown on page 50, there is a definite increase in the average total loss coefficient with turning angle. No assumptions were made concerning velocity profiles, compressibility, or adiabatic flow. These and other assumptions were only necessary to determine the theoretical momentum. A definite dependence of loss coefficient on Reynolds number and Mach number cannot be established from the results obtained. Force plate measurements over a wider range of flow rates may yield such a dependence.

The probe survey results of the 90° bend shown in Figures 22 - 24 raise questions which can only be answered by further investigation. Angular deflections in the lower right corner of Figures 22 and 23 are opposite to the theoretical vortices in Figure 2. The location of the low total pressure loss region in Figure 24 along with a complete absence of loss concentrations in the right upper quarter of the channel seem peculiar. These results may be due to changes in the flow field caused by the probe. Yaw angles and total pressure loss distributions were determined with probes mounted on the upper wall while pitch angles were determined by a probe mounted on the left wall of

Figure 23. Surveys taken by probes mounted on the lower and right walls may yield different results.

APPENDIX A

REDUCTION OF FORCE PLATE MEASUREMENTS

Applying conservation of momentum to the force plate resulted in Equation (4), or:

$$F = \frac{1}{g} \int_{A_2} \rho V_x^2 dA$$

where $g = 32.174 \frac{\text{ft-lbm}}{\text{lbf-sec}^2}$

F = force on the plate in lbf

ρ = density at model exit in $\frac{\text{lbm}}{\text{ft}^3}$

V_x = axial velocity at model exit in $\frac{\text{ft}}{\text{sec}}$

A = cross sectional area at model exit in ft^2

F represents the integration of momentum over the exit plane of the model and is used to determine the following loss coefficient (ζ):

$$\zeta = 1 - \frac{\int_{A_2} \rho V_x^2 dA}{\int_{A_2} \rho V_{th}^2 dA}$$

V_{th} represents the exit velocity that could be achieved from the isentropic expansion shown in Figure 29. Station 1 is shown in Figure 18 and station 2 is at the model exit.

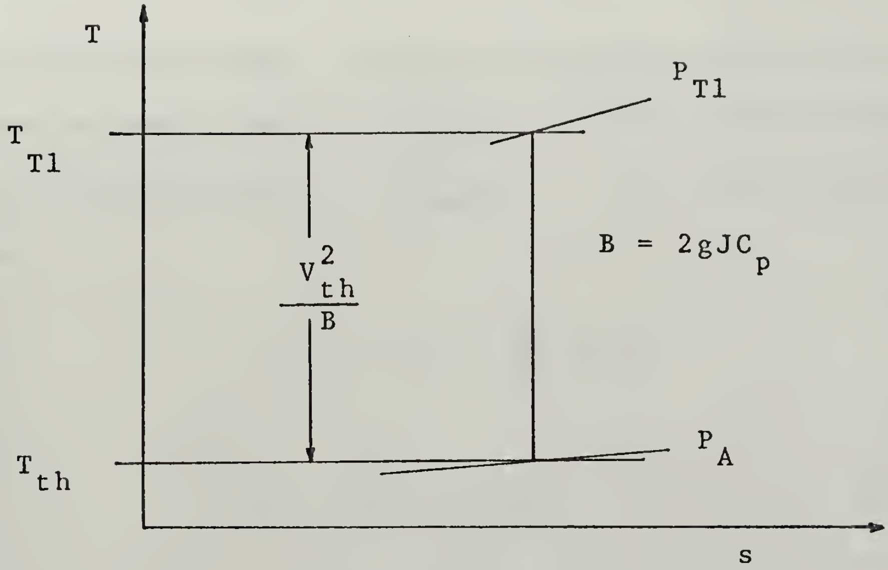

Figure 30

Entropy Diagram for an Isentropic Process

T_{T_1} = total temperature at Station 1 in ^{o}R

P_{T_1} = total pressure at Station 1 in $\frac{lbf}{ft^2}$

P_A = atmospheric pressure in $\frac{lbf}{ft^2}$

T_{th} = theoretical static temperature at Station 2 in ^{o}R

$J = 778.16 \frac{ft\text{-}lbf}{Btu}$

$C_p = 0.24 \frac{Btu}{lbm\text{-}^{o}R}$

T_{T_1} was assumed to be equal to the total temperature measured in the circular pipe. Static pressure at station 2 was assumed to be uniform over the exit plane and equal to atmospheric pressure. Conditions at station 1 were

assumed to be uniform over the channel cross section as were theoretical conditions at station 2. P_1 was determined from the average value of four wall static pressure tap measurements taken at station 1. With these assumptions and measurements, $\int_{A_2} \rho V_{th}^2 dA$ was determined as follows:

$$\dot{m} = \rho_1 A_1 V_1 = \frac{P_1}{RT_1} A_1 V_1 \quad ,$$

where

$$R = 53.34 \; \frac{\text{ft-lbf}}{\text{lbm-}^{\circ}\text{R}} \quad ,$$

$$A_1 = A_2 = \frac{25}{144} \; \text{ft}^2 \quad ,$$

and

$$T_1 = T_{T_1} - \frac{V_1^2}{B}$$

Since

$$\dot{m} = \frac{P_1 A_1 V_1}{R(T_{T_1} - V_1^2/B)} \quad ,$$

$$\frac{\dot{m}R}{B} V_1^2 + P_1 A_1 V_1 - \dot{m}RT_{T_1} = 0$$

and therefore

$$V_1 = \frac{- P_1 A_1 + \sqrt{(P_1 A_1)^2 + \frac{4}{B} (\dot{m}R)^2 \; T_{T_1}}}{\frac{2\dot{m}R}{B}}$$

The isentropic relationship gives

$$P_{T_1} = P_1 \left[\frac{T_{T_1}}{T_1} \right]^{\frac{\gamma}{\gamma-1}} \quad ,$$

where it is assumed that $\gamma = 1.4$

Then,

$$\int_{A_2} \rho V_{th}^2 dA = \rho V_{th}^2 A_2 \quad ,$$

where,

$$\frac{V_{th}^2}{B} = T_{T_1} - T_{th} \quad ,$$

or

$$V_{th}^2 = BT_{T_1} \left[1 - \left(\frac{P_A}{P_{T_1}} \right)^{\frac{\gamma-1}{\gamma}} \right] \quad .$$

Now,

$$\rho_{th} = \frac{P_A}{RT_{th}} = \frac{P_A}{RT_{T_1} \left[\frac{P_A}{P_{T_1}} \right]^{\frac{\gamma-1}{\gamma}}} \quad ,$$

so that,

$$\rho_{th} V_{th}^2 A_2 = \frac{B \left[1 - \left(\frac{P_a}{P_{T_1}} \right)^{\frac{\gamma-1}{\gamma}} \right] P_A A_2}{R \left[\frac{P_A}{P_{T_1}} \right]^{\frac{\gamma-1}{\gamma}}} \quad .$$

The final expression for ζ is therefore:

$$\zeta = 1 - \frac{Fg \; R \left[\frac{P_A}{P_{T_1}} \right]^{\frac{\gamma-1}{\gamma}}}{B \left[1 - \left(\frac{P_A}{P_{T_1}} \right)^{\frac{\gamma-1}{\gamma}} \right] P_A A_2}$$

APPENDIX B

PROBLEMS ENCOUNTERED WITH THE FORCE PLATE APPARATUS AND RECOMMENDATION

The first problem that occurred with the hydraulic force plate apparatus was excessive oil leakage. The O-ring grooves were designed for a rotary O-ring seal. Teflon O-rings were chosen to keep friction between the cylinder and housing as low as possible. The O-rings were ordered from several companies but delivery times were excessive. Rubber O-rings were obtained but failed to provide a good seal. To help solve this problem, a new cylinder was made. The machinist was instructed to omit the O-ring groove and make the piston-cylinder and cylinder-housing clearances as small as possible without restricting rotation. During machining, the inner surface of the housing was found to be slightly out of round. This limited the housing-cylinder clearance while a very close fit was obtained between the piston and cylinder. The apparatus was assembled with an O-ring placed in the housing O-ring groove. An excellent seal was obtained due to the decreased cylinder-housing clearance. The apparatus was tested without the force plate attached and the suction pump was able to handle the oil leakage.

The force plate was attached to the piston and the oil pump and electric motor were turned on. Within a few seconds, the piston was tightly frozen in the cylinder.

The apparatus was disassembled and the piston-cylinder surfaces were badly scored. Apparently, a metal particle became lodged between the two surfaces during rotation. The oil supplied from the pump passed through a filter before entering the apparatus although the type of filter and its condition were not known. The weight of the force plate (ten pounds) produces areas where the piston-cylinder surfaces are forced together. These locations are especially susceptible to scoring due to surface roughness or particles in the oil. The following recommendations are made for further work with the hydraulic force plate apparatus:

1. An investigation be made to determine the type of oil filter system needed.
2. The out-of-round housing be corrected.
3. Clearances between the second cylinder, housing, and piston be maintained.
4. The cylinder O-ring groove in Figure 13A be added to the second cylinder.
5. The rubber O-rings (Porter Seal 568-040 and 568-041, Buna-hardness 70) be used.
6. The piston, cylinder, housing, and back plate be made from materials specified on the original drawings.
7. The force plate be re-designed for minimum weight.
8. The piston-cylinder surfaces be checked for a proper finish especially where holes have been drilled.

BIBLIOGRAPHY

1. Vavra, M. H., Aero-Thermodynamics and Flow in Turbomachines, John Wiley and Sons, 1960.

2. Woods, J. R., An Investigation of Secondary-Flow Phenomena and Associated Losses in a High-Deflection Turbine Cascade, Ph.D. Thesis, Naval Postgraduate School, June 1972.

3. Woods, J. R., The Analytical Treatment of Secondary Flows and Associated Losses in Axial-Flow Turbomachines, Naval Postgraduate School Report NPS-57WO71121A, December 1971.

INITIAL DISTRIBUTION LIST

		No. Copies
1.	Defense Documentation Center Cameron Station Alexandria, Virginia 22314	2
2.	Library, Code 0212 Naval Postgraduate School Monterey, California 93940	2
3.	Chairman, Code 57 Department of Aeronautics Naval Postgraduate School Monterey, California 93940	1
4.	Distinguished Professor M. H. Vavra, Code 57Va Department of Aeronautics Naval Postgraduate School Monterey, California 93940	1
5.	Ensign Paul S. Kenney 831 Appalachee Avenue Winter Park, Florida 32789	1

DOCUMENT CONTROL DATA - R & D

(Security classification of title, body of abstract and indexing annotation must be entered when the overall report is classified)

ORIGINATING ACTIVITY *(Corporate author)*

Naval Postgraduate School
Monterey, California 93940

2a. REPORT SECURITY CLASSIFICATION
Unclassified

2b. GROUP

REPORT TITLE

An Investigation of Secondary Flow Effects
in Curved Channels of Square Cross Section

DESCRIPTIVE NOTES *(Type of report and, inclusive dates)*

Master's Thesis; June 1973

AUTHOR(S) *(First name, middle initial, last name)*

Paul Stephen Kenney

REPORT DATE
June 1973

7a. TOTAL NO. OF PAGES
66

7b. NO. OF REFS
3

. CONTRACT OR GRANT NO.

9a. ORIGINATOR'S REPORT NUMBER(S)

b. PROJECT NO.

c.

9b. OTHER REPORT NO(S) *(Any other numbers that may be assigned this report)*

d.

0. DISTRIBUTION STATEMENT

Approved for public release; distribution unlimited.

1. SUPPLEMENTARY NOTES

12. SPONSORING MILITARY ACTIVITY

Naval Postgraduate School
Monterey, California 93940

3. ABSTRACT

In this study, turbulent flow in a curved channel of square cross section was investigated experimentally to determine secondary flow effects. Probe surveys were conducted to establish vortex and total pressure loss distribution in the exit plane of a 90° bend. Overall losses were determined by measuring the momentum of the flow with a force plate for different Reynolds numbers at turning angles of 0°, 45°, 90°, and 135°.

KEY WORDS	LINK A		LINK B		LINK C	
	ROLE	WT	ROLE	WT	ROLE	WT
Secondary Flow in Square Ducts						
Loss Coefficients						
Force Plate Instrumentation						
Pressure Probe Surveys						

Thesis
K3847 Kenney
c.1
144240
An investigation of secondary flow effects in curved channels of square cross section.